Nucleation Mechanisms and Particle Size Distributions of Polymer Colloids

Enzo Giannetti
Ausimont CRS, Bollate Research Center, 20021 Bollate (MI), Italy

A theoretical model is developed for the time evolution of volume particle size distributions (PSDs) of polymer colloids during the nucleation stage. Analytic expressions for the PSD and related cumulants are presented. Negatively skewed distributions are observed only when the formation rate of mature latex particles is a monotonically decreasing function of time. When this model is tested against experimental PSD data of styrene polymerization at 50°C, agreement between theory and experiment is found only assuming a monotonically decreasing nucleation rate. The fitting is completely missed when the production rate of mature latex particles is predicted according to the coagulative nucleation scheme. Theory and experiment can combine introducing an extended coagulative nucleation model. According to this approach, the nucleation time is much shorter than predicted by earlier theories. As a consequence, most of the mechanistic information convoluted with early-time PSDs is lost.

Introduction

Emulsion polymerization is one of the most important processes for manufacturing synthetic polymers today. The methodology leads to the formation of polymer latexes, sometimes referred to as "polymer colloids." Only a relatively small number of components are required for the reaction. In spite of this apparent simplicity, however, these systems are highly complex involving many chemical and physical processes in as many as three separate phases: the continuous water phase, the polymer particles swollen with monomers, and the monomer droplets. For *ab initio* batch and/or semibatch processes, one of the most complex problems is to understand and describe in detail the mechanisms involved in the birth and growth of latex particles. Many difficulties encountered in modeling the so-called Smith-Ewart (SE) Interval I stem not only from the heterogeneous nature of the system, but also from the intimate coupling to particle growth processes at the very beginning of the reaction. Because mechanistic information is not directly available, it has to be extracted by indirect means. While this aspect constitutes one of the major sources of uncertainty and controversy among researchers, it also represents a challenge in polymer reaction engineering. The complexity of the system, certainly, requires the use of a suitable methodological approach, primarily a *strong physical insight* into the nature of the process that should precede any further attempt to extract information. Nevertheless, to date, a number of different, mutually exclusive mechanisms have been proposed for latex particle formation, including the entry of free radicals into micelles (Harkins, 1947; Smith and Ewart, 1948) and the homogeneous nucleation of oligomeric growing radicals in the aqueous phase (Priest, 1952; Dunn and Chong, 1970; Fitch and Tsai, 1971; Hansen and Ugelstad, 1978). As pointed out by Australian researchers (Lichti et al., 1983; Feeney et al., 1984, 1987a; Napper and Gilbert, 1988, 1990; Casey et al., 1990), in spite of their popularity, both of these two theories were not substantiated by any *unambiguous* experimental evidence. In this light, the same research group (hereafter referred to as the Sydney group) proposed an alternative nucleation scheme, the coagulative nucleation (CN) theory (Feeney et al., 1984, 1987a). According to this multistep mechanism, colloidally unstable "primary" latex particles are formed by homogeneous nucleation. These first-formed "precursor" particles undergo growth mainly by coagulation to form "secondary" precursors of varying coagulation degrees up to a critical level beyond which colloidal stability is reached. The so-formed "mature," colloidally stable latex particles grow then by conversion of monomer to polymer. If operative CN should give rise to a production rate of mature latex particles (denoted by dN_c/dt), it becomes an increasing function of time for much of the nucleation period. Conversely, for any single-step nucleation mechanism, like micellar entry and homoge-

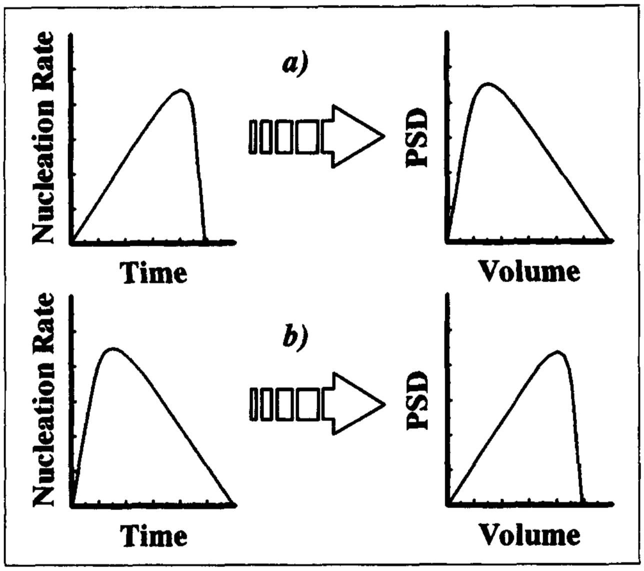

Figure 1. Representative rates of particle formation and their effects on the skewness of resulting PSD: a) coagulative nucleation and b) micellar entry.

neous nucleation, dN_c/dt might reasonably be expected to be a monotonically decreasing function of time. These opposite behaviors led to the idea that the full-volume particle size distribution (PSD) of the latex, immediately after the cessation of particle formation, should provide a more sensitive test for establishing the operative nucleation mechanism in emulsion polymerizations (Napper and Gilbert, 1990). According to this view, any single-step mechanism, like micellar entry, results in a negatively skewed plot of the particle volume distribution, whereas CN predicts a positive skewness (see Figure 1). Experimental PSD data at the end of the SE Interval I from persulfate-initiated emulsion polymerizations using anionic surfactants at concentrations well above CMC (Feeney et al., 1987a, 1987b) were used to support the hypothesis that CN could be operative even in the presence of surfactant micelles. Although other phenomena, like periodic nucleation in unstirred styrene emulsion polymerizations (Feeney et al., 1985) or catalyzed agglomeration during particle nucleation (Schlueter, 1990), agree with a multistep mechanism of particle formation, positively skewed PSDs in the early stage of the reaction have been claimed as one of the most compelling evidence for CN.

In spite of the excellent work of the Sydney Group, there are in our opinion some caveat as to whether the interpretation of the experimental data really suggests CN as providing the best available qualitative and quantitative description of nucleation. These are:

- The shape of the PSD at the end of the SE Interval I was simulated by means of the "zero-one" approximation (Feeney et al., 1984; Napper and Gilbert, 1988). While this simplification has been demonstrated to be accurate enough for describing the kinetic behavior of systems having a low average number of radicals per particle ($\bar{n} < 1/2$), there is no serious analysis as to whether the same approximation could be applied for the description of the time evolution of PSDs as well.
- The robustness of the criterion of positively and/or negatively skewed PSDs at the end of the SE Interval I for discriminating between a single- and multistep nucleation mechanism was not properly addressed due to the lack of analytic relationships between the main operating conditions and the time evolution of PSDs in Interval I.

The main objective of this work is to overcome these limitations and to perform a critical quantitative study of PSDs of polymer colloids during the particle nucleation stage. In this regard, we have recently published a new methodology (Giannetti, 1990) for a comprehensive description of the time evolution of PSDs in the SE Interval II, that is, when the overall number of mature latex particles per unit volume, N_C, remains constant. This new theory is based on an appropriate combination of the Laplace and the generating function transform applied to the constitutive SE population balance equations. Here, we will refer to this model as the generating function (GF) approach. The results obtained represent a substantial improvement vs. the zero-one model in that i) latex particles having more than one growing radical are properly taken into account and ii) general expressions for the time evolution of the cumulants of the PSD are easily available. Moreover, the number density distribution of particles of volume v at time t, $\mathbf{n}_{II}(v,t)$ (subscript II refers to the SE Interval II), is given in terms of a simple convolution integral.

We have now discovered that, with some approximations, the same approach can be easily extended to the nucleation stage of emulsion polymerization. The final results provide analytic expressions for both the number density distribution of latex particles, $\mathbf{n}_I(v,t)$ (subscript I refers to the SE Interval I), and the cumulants of the PSDs. These two theoretical tools are essential for i) extracting mechanistic information from experimental PSDs data and ii) evaluating the sensitivity of the experimental data vs. the operating conditions (initiator and surfactant concentrations, nucleation time, and so on), in relation to the proposed nucleation mechanism. Most (if not all) of the results reported in this article are obtained mainly on the grounds of very simple physical reasonings that always precede any further mathematical modeling. Accordingly, for the better understanding of the concepts developed hereafter, in the next section we will critically compare the GF with the zero-one approach. For simplicity, the analysis is restricted to the SE Interval II. Nevertheless, the results are quite general and can be applied to any interval of emulsion polymerization.

Subsequently, we will show how theories developed for Interval II can be extended to the nucleation stage. The approximations needed for this extension are critically discussed. The theoretical results will be then tested against experimentally available PSD data of styrene polymerization (Lichti et al., 1983). If CN theory is applied in its original formulation (Feeney et al., 1984), the agreement with experimental data is completely missed. On the contrary, experimental and theoretical results can combine assuming that the operative nucleation mechanism incorporates both CN and micellar entry. This extended nucleation mechanism has already been suggested by the Sydney Group (Gilbert et al., 1991), although no further details about its implementation have been reported. Even though the formulation of an alternative particle formation mechanism represents an ancillary problem to the main focus of this article, we will highlight the fact that the problem of particle birth in emulsion polymerization is anything but a consolidated problem.

Generating Function vs. Zero-One Approach

According to Lichti et al. (1982), in an emulsion polymerization the time evolution of the particle size distribution, $\mathbf{n}(v,t)$, is given by the following matrix equation:

$$\frac{\mathbf{n}(v,t)}{\partial t}=\mathbf{\Omega}\ \mathbf{n}(v,t)-\frac{\partial}{\partial v}\left[(v,t)\right]+\mathbf{K}\ \mathbf{n}(v,t)]+\mathbf{c}(v,t) \qquad (1)$$

Here, $\mathbf{n}(v,t)$ is a vector with elements $n_i(v,t)$ which are the relative number densities of latex particles containing i radicals, $\mathbf{\Omega}$ is a square matrix whose elements ij describe the kinetic coupling between n_i and n_j, $\mathbf{K}$ is a diagonal matrix whose nonzero elements $K_{ii}(v,t)$ give the volume growth rate of a particle containing i radicals, and $\mathbf{c}(v,t)$ is a vector whose elements $c_i(v,t)$ give the creation rate of new latex particles containing i radicals at volume v. One common assumption regarding K_{ii} is that $K_{ii} = iK$ where K is the volume growth rate of a particle containing one free radical. Equation 1 is the finite difference form of more general population balance equations common to many engineering problems, describing the time evolution of dispersed multiphase systems, where the dispersed-phase particles continually forego their individual identities through the processes of particle agglomeration and break-up (Ramkrishna, 1985). By dropping the source term $\mathbf{c}(v,t)$, we are restricted to SE Interval II. For systems having a low average number of radicals per particle ($\bar{n}<0.5$) analytic solutions are readily available on the grounds of the so-called instantaneous approximation (zero-one approach). According to this simplification, the behavior of the system is adequately described by only two differential equations out of the whole infinite set represented by the matrix equation (Eq. 1). Since no particle contains more than one growing radical and entry into a particle containing a growing chain causes instantaneous termination (Lichti et al., 1981), we have:

$$\frac{\partial n_o}{\partial t}=-\rho n_o+qn_1 \qquad (2a)$$

$$\frac{\partial n_1}{\partial t}=\rho n_o-qn_1-K\frac{\partial n_1}{\partial v} \qquad (2b)$$

where $q=\rho+k$, and ρ and k are the rate constants for radical entry and exit, respectively.

In the GF approach (Giannetti, 1990) latex particles having any number of growing radicals are considered simultaneously. The methodology lends itself to the description of reacting systems having either high ($\bar{n}>0.5$) or low ($\bar{n}<0.5$) average number of radicals per particle. In the latter case a pseudo-exit rate constant $k^*=(k+2\rho)$ must be introduced. Analytic expressions for $\mathbf{n}_{11}(v,t)$ are obtained by integration of Eqs. 2a and 2b in the zero-one approximation and by solving an associated "wave equation" in the GF model. In both cases, it is assumed that the rate coefficients for radical entry and exit remain constant over the integration interval. Alternatively, ρ, k, and K should be considered suitable averages of the true values over v and t.

While the zero-one approximation is certainly accurate enough to describe the kinetic behavior of a number of reacting systems, like styrene, one must ask whether the same approximation can be applied also to the description of other relevant distributions like PSDs. In emulsion polymerization, a common misinterpretation is the assumption of a substantial equivalence between the kinetics and the time evolution of the PSD. Probably this distortion is nourished by the simple relationship between $\bar{n}_{ss}$ (the average number of radicals at stationary state) and the variation rate of the mean volume of the latex particles, μ_1:

$$\frac{d\mu_1}{dt}=K\bar{n}_{ss} \qquad (3)$$

A more careful analysis shows that this equivalence is apparent and related to simple mass balance and geometric constraints only.

For a better comparison between the zero-one and the GF approach, it is worth focusing, without any loss of generality, on the time evolution of a monodispersed latex of volume V [the associated volume PSD is the Dirac distribution $\delta(v\text{-}V)$]. After a certain reaction time t, in the zero-one approach it will be impossible to find particles having a size larger than $(V+Kt)$. This is not very sound physically since the PSD must be a continuous function of volume in the range $v=V\div\infty$. Actually, even if the associated probabilities are very small for systems with $\bar{n}_{ss}\ll 1/2$, states with a number of radicals $i>1$ are populated. While their contribution is negligible when dealing with the kinetic behavior of the system, this is no longer true for the PSD. The truncation of the volume distribution of the growing particles is an artifact of the zero-one model related to neglecting particles with more than one growing chain. This limitation introduces an error which becomes important at earlier growth times and which propagates heavily when moments (or cumulants) higher than the first one are considered. Mathematically the truncation is represented by the unit step function $U(t\text{-}v/K)$ in the $\mathbf{n}_{11}(v,t)$ function derived under the zero-one approximation (see Appendix A).

The limitations involved in the zero-one model are easily lifted by the GF theory, since allowance is made also for latex particles having more than one growing radical. In principle, this approach should give physically correct answers to the problem. Some limitations still exist and are related to the initial boundary conditions. Simple analytic solutions are achievable only for seeded reactions or for a system whose distribution of radical occupancy is at stationary state at $t=0$. This last condition, however, can be adopted for the extension to SE Interval I without introducing serious errors.

For SE Interval II, some theoretical plotted predictions from the two approaches are reported in Figure 2. Both $\mathbf{n}(v,t)$ and the rate constants are in arbitrary units. The model system has a centered delta Dirac function, $\delta(v)$, as the initial PSD, and its radical distribution is at stationary state. In this example, we set $\rho=k=K=1$. For both approaches, we have: $\bar{n}_{ss}=\rho/(2\rho+k)=0.33$. In the zero-one approximation, however, only two states are allowed, whereas the GF model comprises an infinite number of states with a Poissonian distribution (Blackley, 1982):

$$N_i=\frac{1}{i!}\ (\bar{n}_{ss})^i\exp(-\bar{n}_{ss}) \qquad (4)$$

In Figure 2, the relative amounts of the initial PSDs not yet

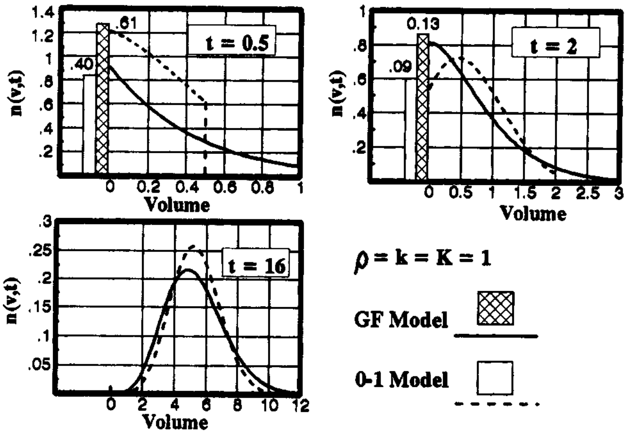

Figure 2. Theoretical PSDs in the Smith-Ewart Interval II.

relaxed at reaction time t are graphically represented by the cross-hatched and empty bars. Their heights are proportional to the area of the unrelaxed monodispersed PSD. The normalized distributions from the two approaches differ considerably, especially at earlier growth times. In this region, the artifact of the PSD truncation distinctive of the zero-one model becomes evident. The difference tends to level off as the growth time increases.

Often, rather than the full PSD, some moments or some particular combinations thereof are needed. While this is impossible for the zero-one model, in the GF approach a simple relationship for the time evolution of the rth cumulant, $k_r(t)$, is available:

$$\Delta k_r(t) = r!\,(\bar{n}_{ss}K/\rho)^r\rho t \tag{5}$$

where $\Delta k_r(t) = k_r(t) - k_r(0)$. Numeric evaluations show that also in the zero-one model the cumulants of the PSD grow linearly with time. As expected, the mean is always the same regardless of the model adopted. On the contrary, both the variance and the skewness increase faster with the GF approach than with the zero-one model. The physical reason for this behavior is the allowance made for latex particles having more than one growing radical. Even if it is negligible, this population grows faster and accounts for $\mathbf{n}(v,t)$ at larger v values. Figure 3 shows the time evolution of the skewness, $k_3(t)$, of the model system adopted for Figure 2. The difference between the two models is not negligible. As a general rule, when K is held constant for any $k_r(t)$ $(r>1)$, the lower $\bar{n}_{ss}$ the smaller is the difference.

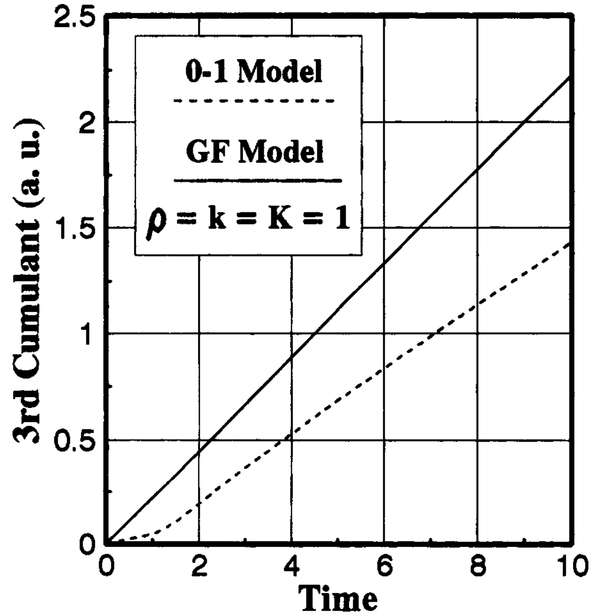

Figure 3. Theoretical time evolution of the skewness of PSD in the Smith-Ewart Interval II.

Extension to SE Interval I

In principle, the PSDs of polymer colloids in Interval I could be obtained from Eq. 1. However, when $\mathbf{c}$ is nonzero, detailed analytic solutions are not available without a number of approximations. These are:

i) All the rate coefficients ρ, k, and K are assumed to be independent of time and volume. Accordingly, under this assumption, kinetic data obtained from PSD are always averages of the true values over v and t. It must be noted here that this is certainly the most critical approximation: the longer the nucleation time, the cruder the assumption will be.

ii) During nucleation, the dN_c population of latex particles formed in the time interval dt is always at equilibrium with respect to its radical state occupancy. Justifications for this conjecture might be twofold: a) $\bar{n}$ is always $\ll 1/2$ due to the relatively rapid exit of monomeric radicals created by chain transfer to monomer; b) in the case of coagulative nucleation, since precursor particles grow very slowly by propagation, coagulation becomes rapid enough for the distribution of free radicals to remain close to its pseudo-steady-state value.

iii) The source term $\mathbf{c}(v,t)$ of the population balance equation is of the form:

$$\mathbf{c}(v,t) = g(t)\mathbf{n}^o(v) \tag{6}$$

In Eq. 6, $g(t)$ is the normalized rate of formation of colloidally stable latex particles, defined as:

$$g(t) = \frac{dN_c(t)}{dt}\Big/N_c(t=\infty) \tag{7}$$

where $N_c(t=\infty)$ represents the stationary number concentration of mature latex particles per unit volume. $\mathbf{n}^o(v)$ is a vector whose elements $n_i^o(t)$ are the relative number densities of newly formed latex particles $dN_c(t)$ containing i growing radicals. Physically, the last assumption means that newly formed particles $dN_c(t)$ have the same PSD throughout all the nucleation period. This simplification seems quite acceptable as long as the $dN_c(t)$ particles are created at volumes reasonably small (Feeney et al., 1984). It is worth pointing out that, according to Eq. 6, all the mechanistic information is sensitive to the rate of particle formation, but not to the shape of the initial volume distribution.

Under the above reported approximations, the extension to Interval I of existing theories of PSDs in Interval II becomes straightforward. To this end, let us focus on a particularly tagged population of particles $dN_c(\tau)$ formed at time $0<\tau<t$. In the absence of agglomeration processes, these particles never lose their own identities. Growth will be mainly by conversion of monomer to polymer. After a certain nucleation time, t, the contribution $d\mathbf{n}_{\rm I}(v,t,\tau)$ of this population to the overall PSD at reaction time t will be:

$$d\mathbf{n}_{\rm I}(v,t,\tau)=g(t)\mathbf{n}_{\rm II}(v,t-\tau)d\tau \tag{8}$$

The overall PSD in Interval I is given by summing up the contributions of all the possible $dNc(\tau)$ populations. This objective is achieved through a simple convolution integral:

$$\mathbf{n}_{\rm I}(v,t)=\int_o^t g(\tau)\mathbf{n}_{\rm II}(v,t-\tau)d\tau=\int_o^t g(t-\tau)\mathbf{n}_{\rm II}(v,\tau)d\tau \tag{9}$$

Of course, the following relationship must be satisfied:

$$\int_o^\infty \mathbf{n}_{\rm I}(v,t)dv=\int_o^t g(\tau)d\tau \tag{10}$$

Physically, Eq. 10 means that the area underneath $\mathbf{n}_{\rm I}(v,t)$ is equal to the number fraction of mature latex particles at time t. At the end of the nucleation time, $t=T$, the PSD becomes normalized. Equation 9 satisfies a more rigorous approach to the problem. Solutions to Eq. 1 are given in terms of the GF approach in Appendix B. This methodology allows the formulation of a more general solution for the $\Psi(x,s,t)$ generating function in SE Interval I:

$$\Psi(x,s,t)=\mathcal{L}^o(s)\exp\left[\frac{\rho}{A}(x-1)\right]\int_o^t g(\tau)\times\exp\left[-\frac{\rho Ks}{A}(t-\tau)\right]d\tau \tag{11}$$

where $\mathcal{L}^o(s)$ is the Laplace transform of the $\mathbf{n}^o(v)$ distribution, s is the Laplace variable conjugate to $v, A=(k+sK)$, and x is a dummy variable associated with the generating function transform. The properties and meaning of the Ψ function are discussed comprehensively in the original work of Giannetti (1990). At the point $x=1$, Ψ reduces itself to the Laplace transform of $\mathbf{n}_{\rm I}(v,t)$:

$$\mathcal{L}[\mathbf{n}_{\rm I}(v,t)]=\mathcal{L}^o(s)\int_o^t g(\tau)\exp\left[-\frac{\rho Ks}{A}(t-\tau)\right]d\tau \tag{12}$$

Of particular interest is the case of $\mathbf{n}^o(v)$ conforming to a Dirac δ function. This situation is representative of PSD data obtained by electron microscopy at the end of Interval I, where the mature latex particles are created at volumes considerably less than the smallest particle observed experimentally. In this situation, $\mathcal{L}^o(s)=1$ so that Laplace transform inversion of Eq. 12 takes the following simpler analytic form:

$$\mathbf{n}_{\rm I}(v,t)=\int_o^t g(t-\tau)\times\left\{e^{-\beta v}\left(\frac{\rho\beta\tau}{v}\right)^{1/2}\mathbf{I}_1[2(\rho\beta v\tau)^{1/2}]+\delta(v)\right\}e^{-\rho\tau}d\tau \tag{13}$$

where $\beta=k^*/K$. Accordingly, under the approximations assumed in this treatment, it is quite evident that the extraction of any mechanistic information from PSDs involves an integral deconvolution problem.

The main success of the simple analysis presented here is the ability to obtain relationships between the time evolution of the PSD and the normalized production rate of mature latex particles where most of the mechanistic information is encapsulated. Single- and/or multistep particle generation mechanisms can be simulated by simple monotonically decreasing and/or increasing nucleation rates or by an appropriate combination of the two. Once $g(t)$ has been specified, $\mathbf{n}_{\rm I}(v,t)$ can be easily obtained from Eq. 13 and the computed PSD compared against experimental data.

Skewness of Early-Time PSDs

According to Napper and Gilbert (1990), the skewness of early-time PSDs provides essential information about the mechanism(s) of particle birth. A negative value should imply that most particles are formed comparatively late in the nucleation period and so have not grown very much. Since the skewness is related to the third moment of the distribution, it seems compelling to work out expressions for the time evolution of these particular averages of the PSD. While this task is not possible with the zero-one model, it becomes straightforward for the GF approach. Actually, in SE Interval I from the Ψ function, we have:

$$\mu_i(t)=\frac{(-1)^i}{\int_o^t g(\tau)d\tau}\left(\frac{\partial^i\Psi}{\partial s^i}\right)_{x=1;\ s=0} \tag{14}$$

In Eq. 14, the integral represents a normalization factor. Another distinctive feature of the GF model is the ability to provide directly also the cumulants of the PSD:

$$k_i(t)=(-1)^i\frac{\partial^i}{\partial s^i}[\ln\Psi]_{x=1;\ s=0} \tag{15}$$

In Eq. 15, the normalization factor is omitted since it never enters the final expression of $k_i(t)$. As is well known the first, second, and third cumulants are the mean, the variance and the skewness of the distribution, respectively. Concerning the time evolution of the mean from the combination of Eqs. 11 and 14 (or 15), we have:

$$\mu_1(t)=\mu_1(0)+\frac{\rho}{\beta}\frac{\int_o^t g(\tau)(t-\tau)d\tau}{\int_o^t g(\tau)d\tau} \tag{16a}$$

Equation 16a can be further recast as follows:

$$\mu_1(t) = \mu_1(0) + \bar{n}_{ss} K \frac{\int_0^t N_c(\tau)d\tau}{N_c(t)} \tag{16b}$$

The integral can be rewritten as $N_c{}^*t$ where $N_c{}^*$ is an averaged value over time t. Accordingly, $\int N_c(\tau)dt/N_c(t)$ is a number representing the effective fraction of latex particles up to reaction time t. The final equation is formally equal to that derived for SE Interval II (Giannetti, 1990):

$$\mu_1(t) = \mu_1(0) + \bar{n}_{ss} K \frac{N_c{}^*(t)}{N_c(t)} t \tag{16c}$$

In principle, from Eq. 15 it is possible to work out relationships for any reaction time t with $0 < t \leq T$, where T represents the end of Interval I. In the sequel, however, we will focus only on time T, since i) it is the PSD at the end of Interval I that is of interest in deciding which mechanism is operative and ii) analytic expressions are comparatively simpler. As discussed in the preceding section, for simplicity, the PSD of newly formed particles is assumed to conform to a centered δ Dirac distribution. If needed, however, this restriction can be lifted making allowance for any distribution. For the time-dependent "source" term $g(t)$, we will consider two representative functional forms which may be proposed for the particle nucleation processes. These are, respectively, a monotonically decreasing and a monotonically increasing normalized rate of production of latex particles:

$$g(t) = \frac{(\nu+1)}{T}(1-z)^{\nu};\ \nu \geq 0 \tag{17a}$$

$$g(t) = \frac{(\nu+1)}{T} z^{\nu};\ \nu \geq 0 \tag{17b}$$

where $z = t/T\,(0 < z \geq 1)$. The Laplace transforms of the related $\mathbf{n}_1(v,t)$ distributions are:

$$\mathcal{L}[\mathbf{n}_1(v,t) = {}_1F_1[\nu+1;\ \nu+2;\ -s\rho T/(s+\beta)] \tag{18a}$$

$$\mathcal{L}[\mathbf{n}_1(v,t) = {}_1F_1[1;\ \nu+2;\ -s\rho T/(s+\beta)] \tag{18b}$$

where ${}_1F_1(a;\ b;\ x)$ denotes the confluent hypergeometric function of variable x with parameters a and b. For a decreasing generation rate of latex particles, at the end of SE Interval I the first three cumulants of the PSD are as follows:

$$k_1(T) = \frac{\rho T}{\beta}\frac{\nu+1}{\nu+2} \tag{19a}$$

$$k_2(T) = \frac{\rho T}{\beta^2}\frac{\nu+1}{\nu+2}\left[2 + \frac{\rho T}{(\nu+2)(\nu+3)}\right] \tag{19b}$$

$$k_3(T) = \frac{2\rho T}{\beta^3}\frac{\nu+1}{\nu+2}\left[3 + \frac{3\rho T}{(\nu+2)(\nu+3)} - \frac{\nu(\rho T)^2}{(\nu+2)^2(\nu+3)(\nu+4)}\right] \tag{19c}$$

For an increasing rate of particle formation, we have:

$$k_1(T) = \frac{\rho T}{\beta}\frac{1}{\nu+2} \tag{20a}$$

$$k_2(T) = \frac{\rho T}{\beta^2}\frac{1}{\nu+2}\left[2 + \frac{(\nu+1)\rho T}{(\nu+2)(\nu+3)}\right] \tag{20b}$$

$$k_3(T) = \frac{2\rho T}{\beta^3}\frac{1}{\nu+2}\left[3 + \frac{3\rho T(\nu+1)}{(\nu+2)(\nu+3)} + \frac{\nu(\nu+1)(\rho T)^2}{(\nu+2)^2(\nu+3)(\nu+4)}\right] \tag{20c}$$

The following main results are immediately obvious:

i) As expected, for $\nu = 0$ (constant nucleation rate) the two sets of equations give the same results.

ii) At the end of Interval I the values of the cumulants depend on the adimensional product ρT only.

iii) Negatively skewed PSDs can be observed only with the decreasing production rate of particles.

Equation 19c agrees with the qualitative reasonings set forth by the Sydney Group. Quantitatively, however, it turns out that PSDs at the end of Interval I become negatively skewed only in a specific region of the adimensional parameter ρT.

$$\rho T > \frac{(\nu+2)(\nu+4)}{2\nu}\left[3 + \left(9 + 12\nu\frac{\nu+3}{\nu+4}\right)^{0.5}\right] \tag{21}$$

For a uniformly decreasing rate of nucleation ($\nu = 1$), negatively skewed PSDs are expected only if $\rho T > 55$. Now, for a certain monomer, the average entry rate constant ρ in Interval I depends on the main operating conditions like initiator and surfactant concentrations, ionic strength, and so on. However, ρ and T are not independent of each other so that the product ρT can be varied over a limited range only. For example, typical values of ρT for styrene span from 10^{-1} up to 10 (Feeney et al., 1984).

Theoretical Predictions

It is interesting to test the theoretical predictions for PSDs in SE Interval I by comparing results from both the zero-one and GF model. As the source term beside a simple monotonically increasing and/or decreasing function as typified by Eqs. 17a and 17b, we will also use the following triangular function:

$$g(t) = \frac{2z}{\alpha T}U(\alpha T - t) + \frac{2(1-z)}{(1-\alpha)T}T(\alpha T, T, t);\ z = t/T \tag{22}$$

where α is a mobile point $(0 < \alpha \leq 1)$; $U(\alpha T - t)$ and $T(\alpha T, T, t)$ are the unit step function and the top hat function, respectively:

$$\begin{aligned} U(\alpha T - t) &= 1,\ t \leq \alpha T \\ &= 0,\ t > \alpha T \end{aligned}$$

$$\begin{aligned} T(\alpha T, T, t) &= 1,\ \alpha T < t \leq T \\ &= 0,\ \text{otherwise.} \end{aligned}$$

Equation 22 is a reasonable approximation for the functional form of the source term $g(t)$ according to the CN theory (Feeney et al., 1984). As an idealized set of kinetic constants,

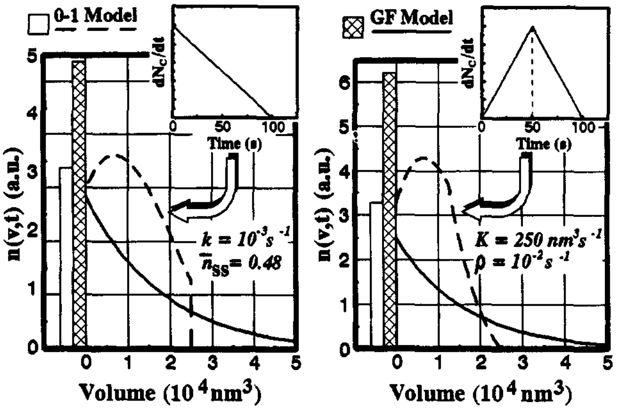

Figure 4. Theoretical PSDs at the end of the nucleation interval.

It assumes uniformly decreasing and a triangular nucleation rate.

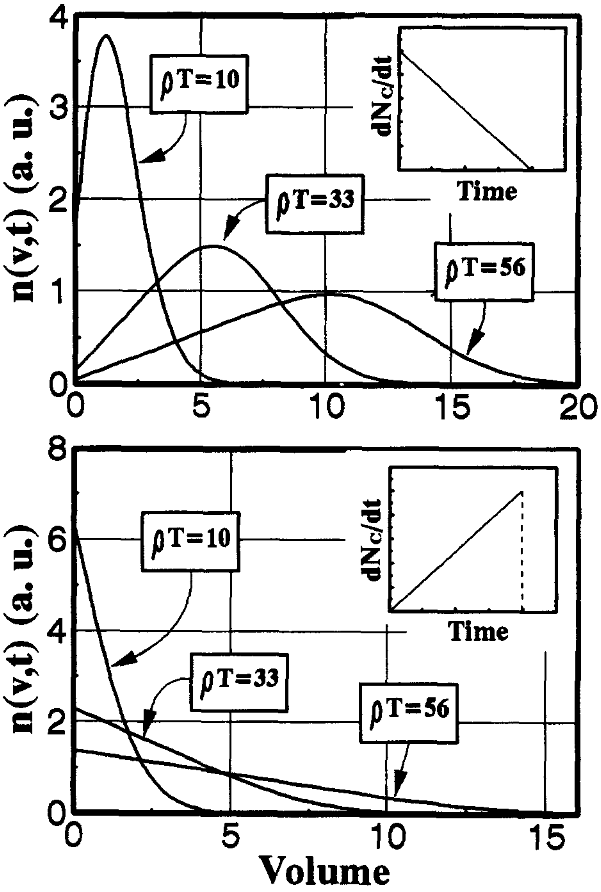

Figure 5. Theoretical PSDs from the GF model.

we choose $K=250\ \mathrm{nm}^3\cdot\mathrm{s}^{-1}$, $\rho=10^{-2}\ \mathrm{s}^{-1}$, and $k=10^{-3}\ \mathrm{s}^{-1}$. This system has a stationary-state average number of radicals $\bar{n}_{ss}=0.48$ and is somehow representative of styrene polymerization. The nucleation time $T=100$ s was used, which again is a reasonable guess for emulsion polymerization of styrene monomer under many practical conditions. Figure 4 shows the results of the simulations with the two approaches. The two bars represent the newly generated monodispersed particles not yet grown by propagation at the end of the nucleation time. The heights of the bars are proportional to the number fraction of these particles. It is apparent that there is a substantial difference between the predictions of the two models.

In the GF approach, the number fraction of latex particles that never experienced radical entry is much higher than that of the zero-one model. The number fraction of newly generated latex particles, which remained unchanged at the end of Interval I, is given by:

$$(1-\bar{n}_{ss})\int_{o}^{T} g(T-t)\exp(-\rho t)dt$$

in the zero-one approximation, whereas the multiplication factor $(1-\bar{n}_{ss})$ is not present according to the GF model. These two quantities approach each other in the limit $\bar{n}_{ss} \ll 0.5$. Concerning the shape of the PSD representing the number fraction of the particles that experienced growth, a dramatic difference results. In the case of a uniformly decreasing nucleation rate (micellar entry) an artifact truncation of the PSD appears with the zero-one approach. When the nucleation rate is represented by a symmetric triangular function this truncation does not appear any longer. This, however, relates only to the shape of the $g(t)$ function. Actually, latex particles of size KT must have grown during all the nucleation period and must have been generated at time $t=0$ where $g(0)=0$. Figure 5 shows some theoretical predictions from the GF approach only. The plots are in arbitrary units for a hypothetical system where $\rho=1$, $\beta=4$ ($k=2$, $K=1$), and $\bar{n}_{ss}=0.25$. PSDs are reported at increasing values of ρT. When $g(t)$ is held constant, the shape of the distribution was found to depend on this product only. The result agrees with Eqs. 19 and 20. On the contrary, the overall PSD depends strongly on the specific functional form of the source term $g(t)$. With a monotonically increasing nucleation rate, most of the latex particles have comparatively small sizes since most of them "appear" quite late and their growth time is considerably shorter than T. On the contrary, with a monotonically decreasing $g(t)$ function an expected "bell shaped" PSD results.

For a uniformly decreasing nucleation rate, Figure 6 reports in arbitrary units the value of the third cumulant of the PSD at the end of Interval I vs. ρT. The curves were evaluated by Eq. 19c for the GF approach ($\beta=4$; $\nu=1$) and numerically (see equations in Appendix A) for the zero-one model. In both cases, however, negatively skewed PSDs are predicted only for relatively high values of ρT. This result is not in agreement with the findings of the Sydney Group. Specifically, in the CN theory $\mathbf{n}_1(v,t)$ was given in terms of a complex equation involving double convolution integrals (Feeney et al., 1984).

Comparison with Experimental Data

Early-time PSD data of styrene polymerization were originally used (Feeney et al., 1984) to support CN mechanism. The experiment was an *ab initio* emulsion polymerization at 50°C. Since the system was not deoxygenated, an induction period of 10 min was observed. The PSD of the latex after 10 min of effective reaction time was positively skewed strongly, and good agreement with experimental data was claimed assuming a nucleation rate arising mainly from coagulation of primary particles. Aggregation rates were provided from a

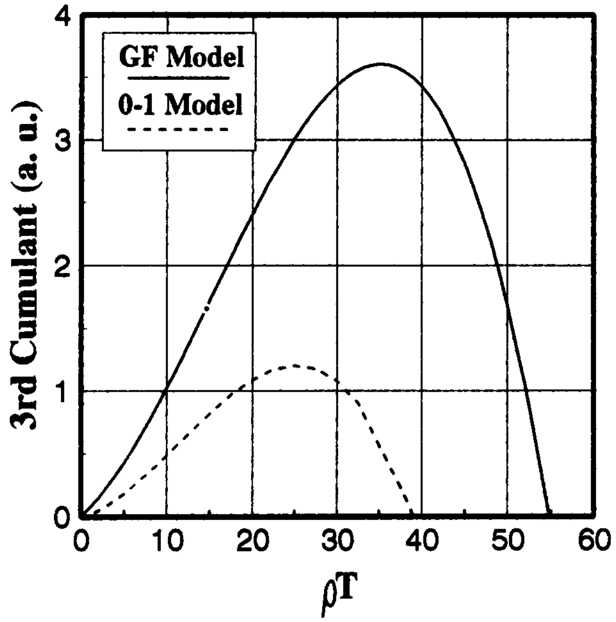

Figure 6. Theoretical time evolution of the skewness of PSDs in the Smith-Ewart Interval I.

combination of extended Müller-Smoluckowski kinetics coupled with DLVO theory. The variation rate of the number density concentration of j-fold precursor particles, Y_j, and of mature particles, N_C, was given as:

$$\frac{dY_j}{dt}=\frac{1}{2}\sum_{i=1}^{j-1} B_{i,j-i}Y_iY_{j-i}-Y_j\sum_{i=1}^{M-1} B_{i,j}Y_i - Y_jB_{M,j}N_C+c(t)\delta_{j,1} \qquad (23)$$

$$\frac{dN_C}{dt}=\frac{dY_M}{dt}=\frac{1}{2}\sum_{i=1}^{M-1}\sum_{j=M-i}^{M-1} B_{i,j}Y_jY_i \qquad (24)$$

where $B_{i,j}$ are the coagulation coefficients between an i-fold and a j-fold flocculated particle, and M is the number of coagulated particles in the smallest, colloidally stable flock. The rate coefficients for coagulation are specified on the grounds of the Müller-Fuchs formulation coupled with DLVO theory:

$$B_{i,j}=\frac{2}{3}\frac{k_BT_e}{\eta W_{i,j}}\frac{(1+r_i/r_j)^2}{r_i/r_j} \qquad (25)$$

where k_B is Boltzman's constant, T_e is the temperature of the emulsion, η the viscosity of the medium, r_j is the radius of the particle, and $W_{i,j}$ is the Fuchs stability ratio. This last quantity was expressed as:

$$W_{i,j}=\frac{r_{11}}{r_{ij}}W_{11}\exp\left[J(r_{ij}-r_{11})\right] \qquad (26a)$$

$$r_{ij}=\frac{2r_ir_j}{(r_i+r_j)} \qquad (26b)$$

and the values of J and W_{11} treated as adjustable parameters.

Table 1. Parameters for Coagulative Nucleation

Symbol	Value	Reference
$c(t)$	$=1.8\times10^{16}$ particles dm^{-3}	This Work
J	$=2.0$ nm^{-1}	Feeney et al. (1984)
M	$=11$	Feeney et al. (1984)
r_1	$=4.0$ nm	Feeney et al. (1984)
T	$=500$ s	Feeney et al. (1984)
W_{11}	$=8.0\times10^{-3}$	Feeney et al. (1984)

The time-dependent nucleation rate relative to the experimental data of Lichti et al. (1983) was simulated with the above model and the values of the rate constants reported in Table 1. These values are exactly the same as those adopted by Feeney et al. (1984), the only difference being $c(t)$. This is due to some minor errors appearing in Eq. 23 in the original article of the Sydney Group. Accordingly, we set $c(t)=1.8\times10^{16}$ particle·dm^{-3} just to have the N_C value as close as possible to the experimental data (5.1×10^{17} particle·dm^{-3}). Figure 7 reports the normalized $g(t)$ source function calculated through the above methodology and the parameters of Table 1. The normalized experimental PSD is also shown as well as the two theoretical PSDs arising from the zero-one and the GF approaches. Contrary to what reported by Feeney et al. (1984), we were not able to fit the experimental data either with the zero-one or the GF model. According to the zero-one approximation, $\mathbf{n}_1(v,t)$ contains single integrals only (see Appendix A). Conversely, the equations derived for the same model by the Sydney Group (Feeney et al., 1984) are quite cumbersome and contain also double convolution integrals. They were obtained specifying $g(t)$ as a triangular function equivalent to Eq. 22 and applying Laplace transform to the

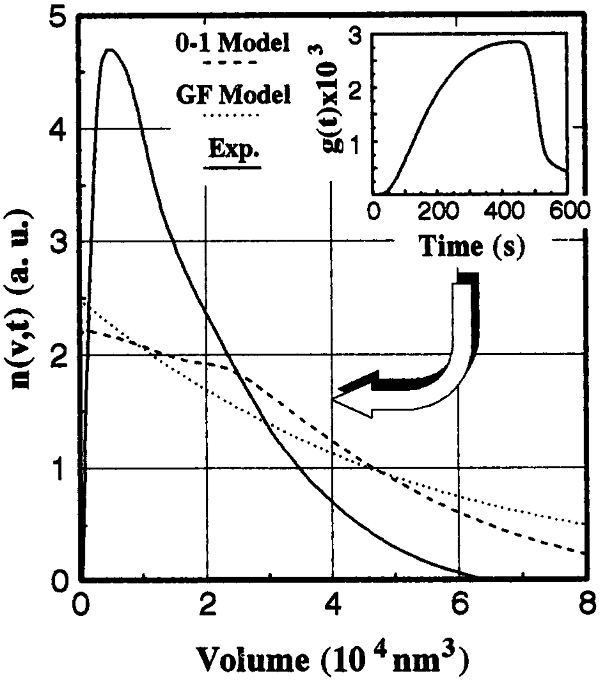

Figure 7. Theoretical vs. experimental early-time PSDs of styrene polymerization: formation rate of latex particles from coagulative nucleation.

system of Eqs. 3a and 3b. We suspect that once the system of the two partial differential difference equations was reduced to a system of ordinary differential equations by Laplace transform, either the solution of this system or, most probably, the integral inversion of the solution itself was not properly performed.

The experimental data of Lichti et al. (1983) are quite nicely fitted assuming a prevailing decreasing rate of formation of mature latex particles (Figure 8). To this end, we adopted as the source term the triangular Eq. 22 setting $\alpha = 0.05$. For the simulation we assumed $\rho = 8.0 \times 10^{-3}\ \mathrm{s}^{-1}$. This value is consistent either with the analysis of the time evolution of PSDs in the SE Interval II (Giannetti, 1990) or with recent theories of radical entry (Maxwell et al., 1991). The growth rate constant K was left unchanged ($K = 220\ \mathrm{nm}^3 \cdot \mathrm{s}^{-1}$). As a consequence, the exit rate constant of free radicals is admittedly much higher ($k = 3.4 \times 10^{-2}\ \mathrm{s}^{-1}$) than in the former article by the Sydney Group, owing to the small size of the latex particles in Interval I. In Figure 8, the theoretical results from both the GF and the zero-one models are plotted in the usual way against experimental data. No attempt was made to fit them by regression analysis; rather, the values of the involved rate constants as well as the shape of the $g(t)$ source term were chosen just to reproduce the early-time PSD of styrene latex. Nevertheless, it is worth noting that these values consistently result in a low average number of radicals per particle ($\bar{n}_{ss} = 0.16$) as expected for SE Interval I of emulsion polymerization of styrene monomer.

The main conclusion which might be drawn from our analysis is that, at least for styrene emulsion polymerization with surfactant concentrations well above CMC, early-time PSDs, when properly analyzed, are in agreement with the formation rate of latex particles being monotonically decreasing (rather than increasing) for much of the nucleation time. Recently, some new experimental data on styrene polymerization became available supporting the hypothesis that, above CMC, micellar entry can significantly contribute to particle formation mechanism (Pearson et al., 1991). Basically, these results agree with the interpretation of the PSD data given here.

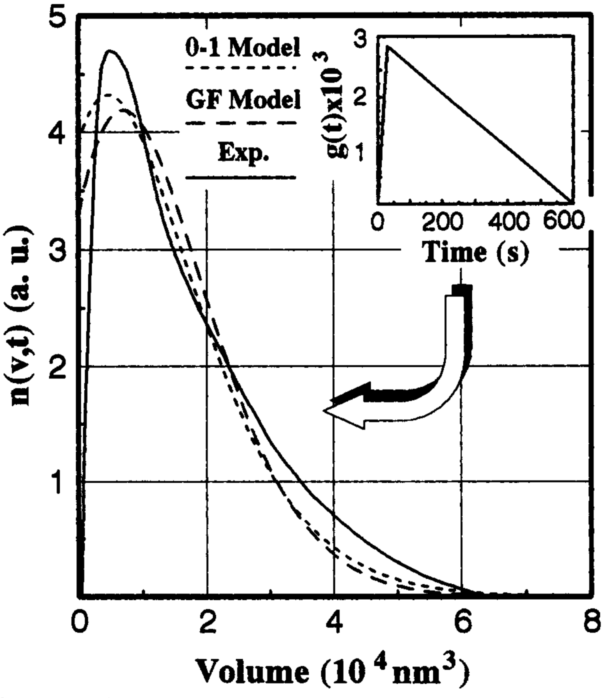

Figure 8. Theoretical vs. experimental early-time PSDs of styrene polymerization.

It assumes decreasing formation rate of latex particles.

Extended Coagulative Nucleation Scheme

The experimental data of Lichti et al. (1983) can be better interpreted in terms of an extended coagulative nucleation (ECN) scheme. This model incorporates features either from micellar and homogeneous nucleation or from CN theory. In this approach, two primary precursor populations are considered: i) particles formed by homogeneous nucleation and ii) precursors formed by micellar entry. One of the main differences between these two populations is the monomer concentration that follows semiempirical equilibrium laws for particles nucleated homogeneously, while it is assumed equal to styrene solubility into surfactant micelles for precursors arising from micellar entry. Another significant difference should be the surfactant associated with these two types of particles. Those formed from micelles would have a significantly higher amount of surfactant. However, as discussed in the next section, there is still a substantial uncertainty on how exactly to model the surfactant distribution between water and unstable precursors. Accordingly, even though not fully respecting the physical behavior of these highly dynamic systems, hereafter we will make use only of equilibrium adsorption isotherms when describing the distribution of amphipathic molecules between water and the polymer surface.

The kinetic model for ECN is as follows. Note that we have neglected reactions in the polymer phase since, as far as nucleation is concerned, mechanistically significant reactions occur mainly in the water phase. Strictly speaking this is not true since exited free radicals should be included into the entry rate coefficient through the associated "fate parameter" (Gilbert and Napper, 1983). This simplification becomes reasonable when the initiator concentration is relatively high: in any case it does not invalidate the basic conclusions of this section. If needed, however, allowance can be easily made also for exited radicals by explicitly introducing the fate parameter (Richards et al., 1989):

Decomposition of initiator:	$\mathrm{I} \xrightarrow{k_d} 2\mathrm{I}^{\bullet}$
Propagation in aqueous phase:	$M_i + M \xrightarrow{k_{pw}} M_{i+1}$
Termination in aqueous phase:	$M_i + T^{\bullet} \xrightarrow{k_{tw}}$ Inert Products
Micellar entry:	$M_i + MC \xrightarrow{k_{me}} Y_{1m}$
Homogeneous precursor formation:	$M_{jcr-1} + M \xrightarrow{k_{pw}} Y_1$
Entry of radicals into particles	$M_i +$ Particle $\xrightarrow{k_e}$ Entry
Coagulative nucleation: $k = 2, \ldots\ldots, M-1$	$Y_i + Y_j \xrightarrow{B_{i,j}} Y_k$

The rates of reactions which enter the material balance are calculated using Eqs. 27-31, according to the above mechanism:

$$R_{iw}=2k_d[\mathrm{I}] \tag{27}$$

$$R_{pw}=k_{pw}[M]_w[T^\bullet]_w \tag{28}$$

$$R_{me}=k_{me}[MC][T^\bullet]_w \tag{29}$$

$$R_{ew}=k_e\frac{N_c}{N_A}[T^\bullet]_w \tag{30}$$

$$R_{tw}=2k_{tw}[T^\bullet]_w^2 \tag{31}$$

$[T^\bullet]_w$ represents the total radical concentration in the water phase, $[MC]$ is the molar concentration of surfactant micelles, and $[M]_w$ is monomer concentration in the water phase. In Eq. 31, the termination rate contains factor 2 in agreement with the IUPAC notation for bimolecular termination between like species. The following steady-state radical balance was used to calculate $[T^\bullet]_w$:

$$2R_{iw}=R_{tw}+R_{ew}+R_{me} \tag{32}$$

If the expressions for each specific rate are substituted into Eq. 32, the aqueous-phase radical concentration can be calculated by solving a simple quadratic equation:

$$[T^\bullet]_w=\frac{-\lambda+(\lambda^2+16\,k_dk_{tw}[\mathrm{I}])^{1/2}}{4k_{tw}} \tag{33a}$$

$$\lambda=k_e\frac{N_c}{N_A}+k_{me}[MC] \tag{33b}$$

The entry rate coefficient was calculated according to the approach of Richards et al. (1989).

$$\frac{1}{k_e}=\frac{1}{k_e^{\max}}+\frac{1}{4\pi r_p^2k_m+\beta_eB_{1,M}N_A} \tag{34}$$

In Eq. 34, $k_e^{\max}$ is a maximum limiting value of the rate coefficient, k_m is surface mass-transfer coefficient, and $(\beta_eB_{1,M}N_A)$ is a term representing bulk diffusion/electrostatic attraction/repulsion of an oligomer with a latex particle of radius r_p. The rate coefficient for free radical capture by micelles, k_{me}, can be estimated assuming a diffusion model as proposed by Hansen and Ugelstad (1978):

$$k_{me}=4\pi r_mD_w\,N_A \tag{35}$$

Here r_m is the average radius of a micelle, and D_w is the diffusion coefficient of free radicals in the aqueous phase. The micelle concentration is related to the overall emulsifier concentration $[S_t]$ through the following relationship:

$$[MC]=\frac{[S_t]-S_p-\mathrm{CMC}}{\bar{n}_{\mathrm{Agg}}} \tag{36}$$

S_p represents the amount of surfactant per unit volume adsorbed onto the polymer surface, CMC is the critical micellar concentration, and $\bar{n}_{\mathrm{Agg}}$ is the mean aggregation number of a micelle.

The formation rate of homogeneous primary precursors, $c_h(t)$ was derived following the well-known HUTF theory (Hansen and Hugelstad, 1978):

$$c_h(t)=(\alpha_{pw})^{jcr}R_{iw}N_A \tag{37a}$$

$$\alpha_{pw}=\frac{R_{pw}}{R_{pw}+R_{ew}+R_{mw}+R_{tw}} \tag{37b}$$

In Eq. 36a, j_{cr} represents the critical chain length for homogeneous nucleation, and α_{pw} is the probability of propagation of a radical species in the water phase. Finally, the variation rate of the density of the k-fold precursors, Y_k, is given by the following set of ordinary differential equations that account for the birth and death by coagulation as well for growth by propagation (Richards et al., 1989).

Micellar Primary Precursors:

$$\frac{dY_{1m}}{dt}=N_AR_{mw}-B_{1m,1m}(Y_{1m})^2 - Y_{1m}\sum_{i=1}^{M-1}B_{i,1m}Y_i-B_{1m,M}N_CY_{1m}-G_{1m}Y_{1m} \tag{38}$$

Homogeneous Primary Precursors:

$$\frac{dY_1}{dt}=c_h(t)-B_{1,1m}Y_1Y_{1m}-Y_1\sum_{i=1}^{M-1}B_{1,i}Y_i -B_{1,M}N_CY_1-G_1Y_1 \tag{39}$$

k-Fold Precursors:

$$\frac{dY_k}{dt}=\frac{1}{2}\sum_{i=1}^{k-1}B_{i,k-i}Y_iY_{k-i}+B_{1m,k-1}Y_{1m}Y_{k-1} +\frac{1}{2}B_{1m,1m}Y_{1m}Y_{1m}\delta_{k,2}-Y_k\sum_{i=1}^{M-1}B_{k,i}Y_i -B_{k,1m}Y_kY_{1m}+G_{1m}Y_{1m}\delta_{k,2}+G_{k-1}Y_{k-1}-G_kY_k -B_{M,k}N_CY_k \tag{40}$$

Mature Latex Particles:

$$\frac{dN_c}{dt}=\frac{1}{2}\sum_{i=1}^{M-1}Y_i\sum_{k=M-i}^{M-1}B_{i,k}Y_k +B_{1m,M-1}Y_{1m}Y_{M-1}+G_{k-1}Y_k-B_{M,M}N_C^2 \tag{41}$$

In Eqs. 38-41, the subscripts $1m$ and 1 refer to micellar and homogeneous primary precursors, respectively. G_k is given as:

$$G_k=\bar{n}\frac{k_pC_{Mk}M_o}{N_Ad_pV_p} \tag{42}$$

where $\bar{n}$ is the average number of free radicals per precursor particle, k_p is the propagation rate coefficient, C_{Mk} is the monomer concentration inside a k-fold precursor, M_o is the molecular weight of the monomer, and V_p is the volume of a newly formed precursor particle. According to Richards et al. (1989), C_{Mk} is given by:

$$C_{Mk} = C_M \tanh\left(\frac{k^{1/3} r_1}{r_{FH}}\right) \tag{43}$$

The hyperbolic tangent term accounts for the variation of monomer concentration inside precursor particles with radius $r_k = k^{1/3} r_1$. In Eq. 43, C_M is the large-radius-limiting saturated monomer concentration, and r_{FH} is a "Flory-Huggins radius" (Feeney et al., 1987a). For micellar primary precursors, C_{M1m}, rather than through Eq. 43, is found from the micellar dimension and the monomer solubility within the micelle itself.

The coagulation rate coefficients $B_{i,j}$ are calculated through Eq. 25 using the Fuchs formulation coupled to DLVO theory as reported by Richards et al. (1989). Strictly speaking, the population balance equations (Eqs. 38–40), describing the time evolution of precursor particles, are coupled to the developing PSD of mature latex particles through the coagulation kernel $B_{i,M}$. In our approach, rather than using the full PSD, the size of mature latex particles was calculated by Eq. 16b. Furthermore, the contribution of the surfactant formed *in situ* by water-phase termination is neglected in this particular case, where ECN is applied for the simulation of an emulsion polymerization with surfactant concentration well above CMC.

At this juncture, it is worth noting that the distribution of the surfactant between the polymer surface and the water phase is calculated by the Langmuir adsorption isotherm either for a j-fold precursor or for a mature latex particle.

$$N_s = \frac{A_t}{a_s(1 + b_s^{-1}[S_w]^{-1})} \tag{44}$$

Here N_s is the total number of surface sites occupied by surface-active species, A_t is the total area of precursors plus latex particles, $[S_w]$ is the concentration of the surface active species in the water phase, a_s is the area occupied by a surfactant molecule adsorbed onto the polymer surface, and b_s is a constant depending on the surfactant and the surface. $[S_w]$ can be calculated by mass balance and Eq. 44 from the total amount of surfactant per unit volume of water phase, $[S_t]$ (Feeney et al., 1987a), while the total area of precursors plus latex is given by:

$$A_t = \sum_{i=1}^{M-1} 4\pi r_i^2 Y_i + 4\pi r_{1m}^2 Y_{1m} + 4\pi r_p^2 N_c \tag{45}$$

where r_p is calculated by Eq. 16b.

The formation rate of micellar precursors, R_{mw}, requires the knowledge of both the dimension and the aggregation number of the micelles under reaction conditions. As is well known, the shape, the CMC, and the aggregation number of anionic surfactants are influenced strongly by the presence of added electrolytes in the solution as well as of a second liquid phase. Fortunately, the data of Lichti et al. (1983) refer to an emulsion polymerization in the presence of SDS surfactant. This micelle forming substance is one of the most thoroughly investigated in the scientific literature so that a large number of CMC data are available between 20 and 50°C. Within this temperature interval, CMC does not vary very much in pure water. According to a simple micellar equilibrium theory (Hiemenz, 1986), for a 1:1 anionic surfactant a double logarithmic plot of the activity of the amphipathic moiety, a_{CMC}, vs. the activity of the overall concentration of cationic species at equilibrium, a_{CMC+S}, should result in a straight line of slope $(1-\alpha)$, where α is an "average fraction of ionization." Figure 9 shows a plot for SDS. Experimental data were taken from literature and cover a wide range of ionic strength. The activity coefficients of the ionic species were calculated by the Davies equation:

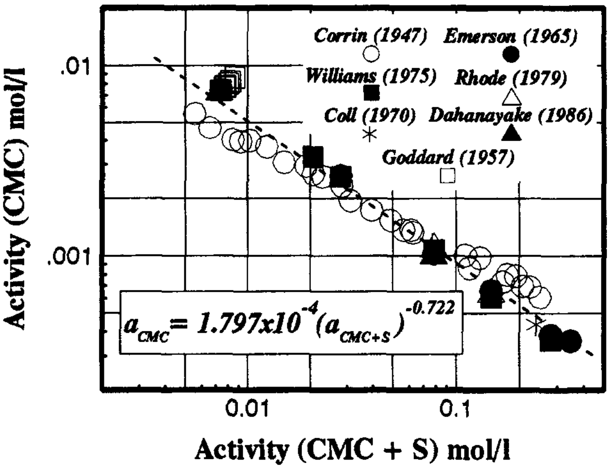

Figure 9. Activity of SDS at CMC vs. activity of the overall concentration of cationic species in the aqueous solution.

$$-\log \gamma_{\pm} = A z_{\pm}\left(\frac{I^{1/2}}{1+I^{1/2}} - 0.02\, I\right) \tag{46a}$$

$$A = 1.825 \times 10^6 (\epsilon_o \epsilon_r T_e)^{-3/2} \tag{46b}$$

where $\epsilon_o \epsilon_r$ is the permittivity of the medium and I the ionic strength defined as:

$$I = \frac{1}{2}\sum_i z_i^2 C_i \tag{47}$$

In Eq. 47, z_i is the valence number on the ith species whose concentration is C_i. A nice correlation was found with $\alpha = 0.27$ in good agreement with the suggested average fraction of ionization $\alpha = 0.25$ of anionic surfactants (Hiemnez, 1986). Different techniques are used for the determination of the micellar aggregation number, $\bar{n}_{\mathrm{Agg}}$. As a general rule, the addition of neutral electrolytes to solutions of ionic surfactants in aqueous solutions causes an increase in the aggregation number. Again, in Figure 10, we report a double logarithmic plot of $\bar{n}_{\mathrm{Agg}}$ vs. the activity of the overall cationic species present at equilibrium.

Normally, water insoluble compounds, like styrene monomer, may be solubilized in the micelle. This phenomenon causes an increase in the aggregation number until the solubilization limit is reached. A reasonable estimate of the sol-

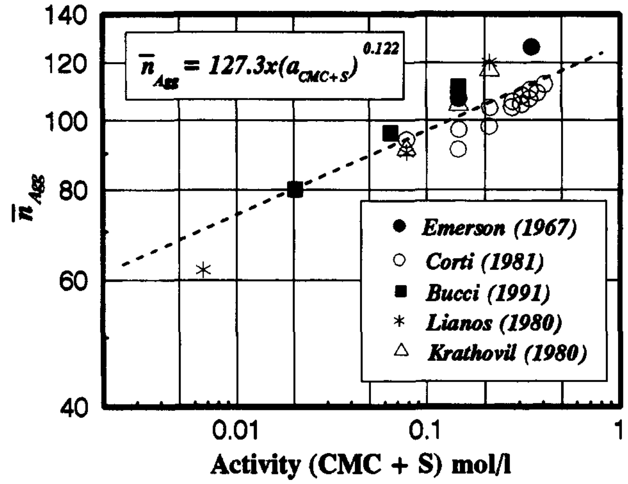

Figure 10. Average micellar aggregation number of SDS vs. activity of the overall concentration of cationic species in the aqueous phase.

ubility of the styrene monomer in SDS micelles can be found in the work of Almgren et al. (1979). According to the proposed model, the mean number of solubilized A molecules per micelle, X_A, is given by:

$$X_A = K_{eq}[A]_w \tag{48}$$

where $[A]_w$ is the water concentration of solubilized molecules at equilibrium with micelles. K_{eq} has been determined for a large number of aromatic compounds and a good correlation was found between this equilibrium constant and the normal boiling temperature of the solubilized molecule. Finally, the increase of the micellar aggregation number, $\Delta\bar{n}_{Agg}$, resulting from the addition of X_A molecules to micelles with aggregation number $\bar{n}_{Agg}$, is easily evaluated by equating the micelle area per head group before and after addition (Almgren, 1991):

$$\Delta\bar{n}_{Agg} = 2X_A \frac{V_A}{V_s} \tag{49}$$

where V_s and V_A are the hydrophobic volumes of the surfactant tail and the additive A, respectively. From all the above reported correlations and equations, it is now possible to find either micelle concentration or micellar radius under reaction conditions and, consequently, R_{ew}. Furthermore, under the assumption of volume additivity, the monomer micellar concentration can be easily calculated. Such a concentration is experienced by free radicals entering aqueous micelles to form a micellar primary precursor. Consequently, C_{M1m} is set equal to the monomer concentration within micelles at equilibrium.

The final aspect explicitly incorporated in ECN theory is the the interaction between the surfactant (SDS) and the initiator (KPS). Recently, Okubo and Mori (1990, 1991) reported some evidences according to which SDS affects the rate of KPS decomposition. It was demonstrated that only free SDS molecules dispersed in the water phase have the ability to accelerate KPS decomposition, while surfactant molecules adsorbed onto the polymer particles are ineffective. The data of Okubo and Mori are redrawn in Figure 11. The following simple relationship is found:

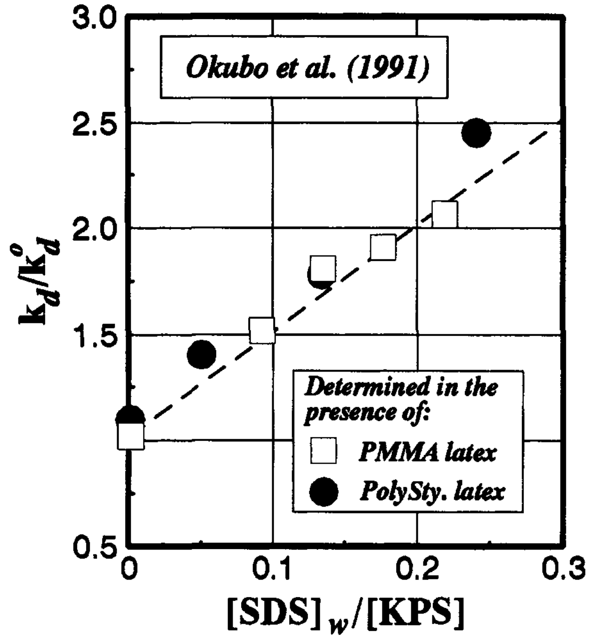

Figure 11. Influence of concentration in the aqueous phase of free SDS molecules on the decomposition rate constant of dissolved KPS.

$$k_d/k_d^o = 1 + 5\,\frac{[S_w]}{[I]} \tag{50}$$

In Eq. 50, k_d^o is the decomposition rate constant in the absence of added surfactant molecules. R_{iw} becomes thus coupled to the SDS mass balance.

The preceding system of population and mass balance equations constitutes the core of the ECN theory and form a stiff set of nonlinear algebraic and differential equations. Appropriate algorithms were used for the numerical integration. In the following, all the simulations were made using 10 bytes floating-point variables according to IEEE 754 standard. Parameters needed for the computations were obtained from the literature: values and related references are given in Table 2.

The data of Lichti et al. (1983) refer to a styrene polymerization at 50°C with $[I] = 1.52\times10^{-2}$ mol·dm^{-3} KPS and $[S_t] = 2.66\times10^{-2}$ mol·dm^{-3} SDS. The first determination of PSD was after 10 min of effective reaction time. Other determinations were after 15, 20 and 25 min, respectively. To fit the PSD data of the first latex sampling (10 min), the rate constants ρ and β were initially determined from the first two cumulants of the distribution using Eq. 5. In the ECN scheme, these two rate constants are needed for estimating the average growth rate $\bar{n}K$ that enters the precursor population balance equations through the coupling of the $B_{i,M}$ coagulation kernels to the PSD of mature latex particles. With this first estimate, the source term $g(t)$ is then generated and the experimental PSD fitted by nonlinear least-square (NLLS) regression of the ρ and β rate constants. The overall procedure is then repeated until convergence, which is achieved generally after two or at least three iterations.

Table 2. Parameters for ECN Simulations

Symbol	Value	Reference
	Parameters for Styrene at 50°C	
C_M	$=5.1\ \mathrm{mol\cdot dm^{-3}}$	Lichti et al. (1983)
d_M	$=924\ \mathrm{g\cdot dm^{-3}}$	Patnode and Scheiber (1939)
d_p	$=1{,}084\ \mathrm{g\cdot dm^{-3}}$	Patnode and Scheiber (1939)
D_w	$=2.86\times10^{10}\ \mathrm{dm^2\cdot s^{-1}}$	Hansen and Ugelstad (1978)
k_p	$=258\ \mathrm{dm^3\cdot mol^{-1}\cdot s^{-1}}$	Gilbert and Napper (1982)
k_{pw}	$=258\ \mathrm{dm^3\cdot mol^{-1}\cdot s^{-1}}$	Maxwell et al. (1991)
k_{tw}	$=3.7\times10^{9}\ \mathrm{dm^3\cdot mol^{-1}\cdot s^{-1}}$	Maxwell et al. (1991)
$[M]_w$	$=4.3\times10^{-3}\ \mathrm{mol\cdot dm^{-3}}$	Lane (1946)
V_A	$=197\ \mathrm{\AA^3}$	This Work
	Parameters for KPS	
k_d^{o}	$=1.0\times10^{-6}\ \mathrm{s^{-1}}$	Behrmans and Edwards (1980)
	Parameters for SDS at 50°C	
a_s	$=43\ \mathrm{\AA^2\cdot molecule^{-1}}$	Ahmed et al. (1980)
b_s	$=2{,}400\ \mathrm{dm^3\cdot mol^{-1}}$	Ahmed et al. (1980)
C_{M1m}	$=1.66\ \mathrm{mol\cdot dm^{-3}}$	This Work
CMC	$=4.4\times10^{-3}\ \mathrm{mol\cdot dm^{-3}}$	This Work
K_{eq}	$=1.68\times10^{4}\ \mathrm{mol^{-1}}$	This Work
$\bar{n}_{Agg}$	$=162$	This Work
r_m	$=2.58\ \mathrm{nm}$	This Work
V_S	$=385\ \mathrm{\AA^3}$	Almgren and Swarup (1982)
	Parameters for Micellar and Coagulative Nucleation	
H	$=6.5\times10^{-21}\ \mathrm{J}$	Ottewill (1982)
j_{cr}	$=4$	Maxwell et al. (1991)
k_e^{max}	$=2.0\times10^{8}\ \mathrm{dm^3\cdot mol^{-1}\cdot s^{-1}}$	Richards et al. (1989)
k_m	$=10.\times10^{-8}\ \mathrm{m\cdot s^{-1}}$	Richards et al. (1989)
M	$=21$	Richards et al. (1989)
r_{FH}	$=15\ \mathrm{nm}$	Feeney et al. (1987a)
r_1	$=1\ \mathrm{nm}$	Richards et al. (1989)
β_e	$=1$	Richards et al. (1989)
δ	$=1.41\ \mathrm{\AA}$	Feeney et al. (1987a)
ϵ_o	$=8.85\times10^{-12}\ \mathrm{C^2\cdot J^{-1}\cdot m^{-1}}$	Perry (1984)
ϵ_r	$=69.9$	Perry (1984)
η	$=3.0\times10^{-4}\ \mathrm{kg\cdot m^{-1}\cdot s^{-1}}$	Perry (1984)
ω	$=1$	Richards et al. (1989)

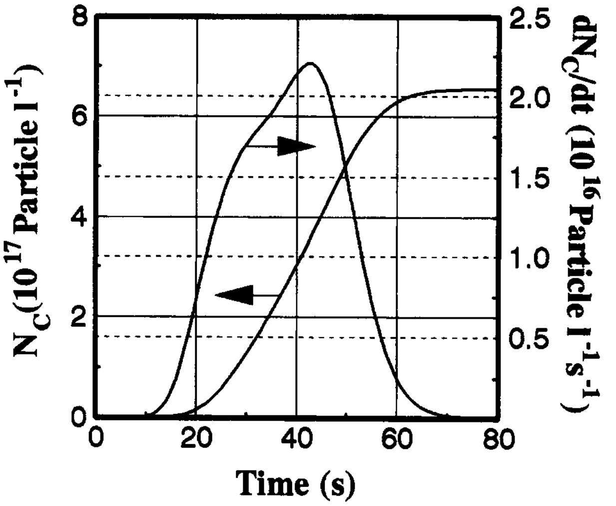

Figure 12. Rate of formation and number concentration of latex particles of styrene emulsion polymerization according to ECN theory.

Figure 12 shows a plot of the time dependence of both dN_C/dt and $N_C(t)$ computed by numerical solution of Eqs. 38–41. The experimental final particle number (5.1×10^{17} particle $\mathrm{dm^{-3}}$) is reproduced to within 30%. Noticeably, ECN gives nucleation rates considerably faster than those calculated neglecting micellar entry. Nucleation of new latex particles is completed within 70–80 s, while the SE formula gives an estimate of T of about 500 s. Figure 13 shows the number density of both micellar and homogeneous primary precursors. The sudden decrease in the number of micellar precursors coincides with the disappearance of micellar soap. At the same time, the formation rate of homogeneous primary precursors increases sharply up to a nearly constant value. The maximum number of homogeneous precursors, however, is always two orders of magnitude lower than that of micellar precursors in the presence of micellar soap. Figure 14 shows the PSD at $t=600$ s computed by ECN theory (dotted line) with ρ and β rate constants chosen to best fit experimental data (full line). Although some distortions are present, the fitting looks quite satisfactory in view of all the approximations which have been made.

Through the NLLS fitting methodology outlined above, the values of the rate constants averaged over Interval I were $\rho=7.3\times10^{-3}\ \mathrm{s^{-1}}$ and $\beta=2.45\times10^{-4}\ \mathrm{nm^{-3}}$. These numbers give an average growth rate $\bar{n}K=29.8\ \mathrm{nm^3\cdot s^{-1}}$. It is interesting to compare the rate parameters of Interval I with those obtained in Interval II from the experimental PSDs at 15, 20 and 25 min, respectively. It must be recalled, however, that the procedure is intrinsically affected by a severe error propagation. Actually, once the experimental diameter PSD (by electron microscopy) is converted to volume PSD, inevitably a considerable amplification of the involved errors occurs. For example, according to the GF theory (Giannetti, 1990) $\bar{n}K=\Delta k_1/\Delta t$ and $\rho=2/\Delta t(\Delta k_1^2/\Delta k_2)$. If the accuracy of the electron microscopy experiment is ϵ, $\bar{n}K$ and ρ could be determined with a precision of 3ϵ and 12ϵ, respectively. For the experiment of Lichti et al. (1983), ϵ was ±3%.

Figure 15 shows the values of ρ and $\bar{n}K$ averaged over two consecutive latex samplings, as a function of time. For Interval

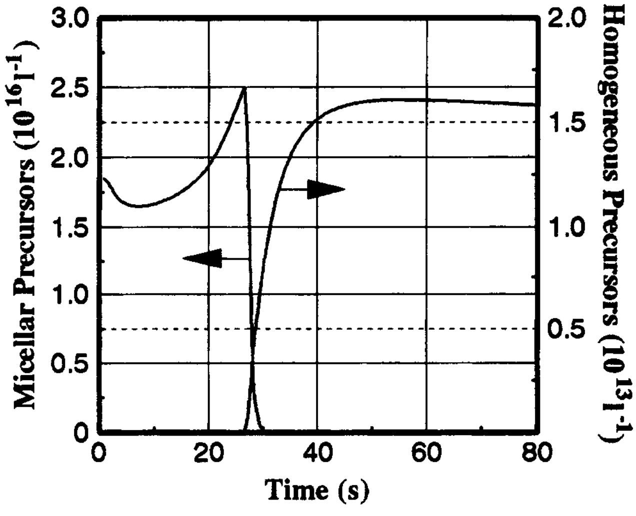

Figure 13. Number density of micellar and homogeneous primary precursors during styrene emulsion polymerization according to ECN theory.

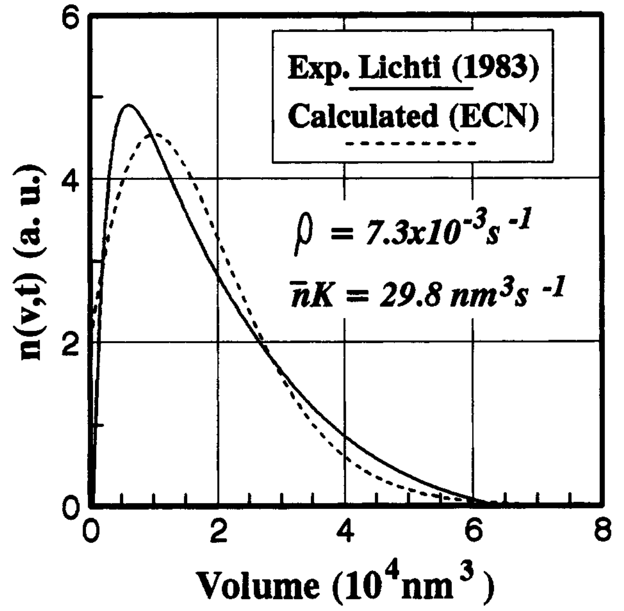

Figure 14. Theoretical (ECN theory) vs. experimental early-time PSDs of styrene polymerization.

II, we adopted the methodology reported in our previous work (Giannetti,1990). In this case, however, to achieve a higher precision (as well as correcting some minor misprints in the previous reference), rather than approximating the initial PSD with a $\Gamma(v)$ distribution, we used the full experimental PSD data. Within experimental errors, the entry rate constant does not vary with conversion as predicted by recent theories on radical entry mechanisms (Maxwell et al., 1991). On the contrary, the average growth rate is definitely much lower in Interval I than in Interval II. This observation is consistent with the more rapid exit during the nucleation stage of monomeric free radicals arising from transfer to monomer.

Certainly, the most relevant feature of the ECN model is the prediction of nucleation times much shorter than expected either by the SE or the CN theory. Since all the mechanistic information of early-time PSDs is convoluted with this distribution according to Eq. 13, a problem arises as to whether this set of experimental data is sensitive enough to any mechanistic fine detail. Actually, immediately after the cessation of nucleation, the content of information embedded into PSDs weakens very quickly owing to the stochastic broadening arising from particle growth by conversion of monomer to polymer. The data of Lichti et al. (1983) at $t = 600$ s might thus be fitted either with a prevailing increasing or prevailing decreasing nucleation rate with ρ and β parameters being within a physically reasonable range of values. Apparently, only the measurements of PSDs at very early reaction times could significantly elucidate the mechanism(s) of particle formation. This, however, poses a number of experimental difficulties involved in the determination of very small particles by special techniques such as neutron scattering (Feeney et al., 1988).

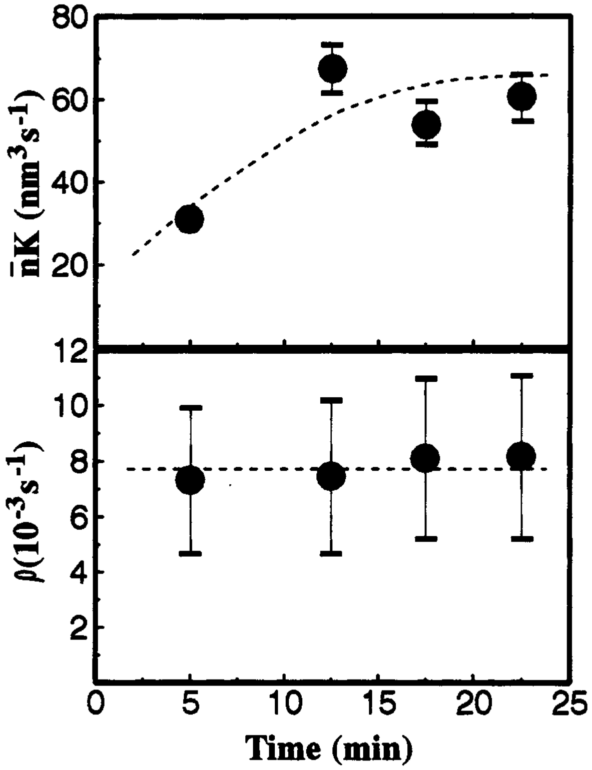

Figure 15. Averaged values of rate parameters of styrene emulsion polymerization from PSD data analysis according to the GF model.

Limitations and Future Developments

Basically, the ECN scheme should be considered a straightforward extension of previous models like the HUTF and the CN theory. In all these approaches, the fate of the precursor particles is detailed in terms of their relative stabilities according to theories of colloidal science. This approach certainly has the advantage of a more solid theoretical footing than the original nucleation scheme of Harkins and Smith-Ewart. However, little attention has been paid to possible limitations of this theoretical body in the description of the behavior of very small and unstable particles under highly dynamic conditions. This applies especially to the surfactant whose role is often more complex than simply determining the overall number of latex particles. Specifically, the adsorption of the surfactant on the particle surface influences the coagulation rate coefficients between precursor particles. Adsorption isotherms are used to determine the surfactant concentration on the polymer. This value, however, refers to equilibrium conditions and does not properly take into account the dynamic nature of both the adsorption process and the coagulation between unstable precursors. Accordingly, when modeling the aggregation process during the nucleation stage, a problem of general nature concerns the surfactant distribution as well as the micellar soap balance. The surface coverage factor Θ_s can be easily found by rearranging the Langmuir isotherm (Eq. 44)

$$\Theta_s = \frac{k^*[S_w]}{1 + k^*[S_w]} \tag{51}$$

where $k^* = K_{\mathrm{Surf}}/\omega$. Here ω is the molar concentration of water (55 $\mathrm{mol \cdot L^{-1}}$) and K_{Surf} describes the adsorption equilibrium between water soap, S, and a latex particle, P:

$$S+P \underset{k_+}{\overset{k_-}{\leftrightarrows}} S_p;\ K_{\text{Surf}}=k_+/k_-$$

For SDS, at 50°C, $K_{\text{Surf}}=1.32\times 10^5$. The desorption rate of ionic surfactants from polymer surfaces is known as an extremely slow process; for example, k_- of SDS from nylon is 3.7 s^{-1} (Lang and Zana, 1987). Accordingly, the adsorption rate of SDS onto polystyrene particles should be higher than the desorption rate by at least three orders of magnitude. This value agrees with the common experience in polymer latex technology, where surfactant adsorption is known as a very fast and energetically favorable phenomenon. In turn, the lifetime of the aggregation process of the precursor particles is:

$$\tau_{\text{Agg}}=(2\ B_{i,j}Y_i)^{-1} \tag{52}$$

To the first approximation, the number concentration of Y_i particles could be set at the same level as the generation rate of free radicals. Numerically, under the reaction conditions adopted in the previous section for styrene polymerization, the lifetime of aggregation for most of the j-flock precursors is not negligible with respect to the overall nucleation time.

When this last consideration is coupled with the surfactant adsorption rate (that, at least within the time-frame of the nucleation stage, should be considered as an irreversible process), it turns out that the surface coverage of the precursor particles cannot be evaluated from a simple equilibrium isotherm. Rather, to properly account for the fate of the adsorbed surfactant and, by implication, for the colloidal stability of the precursor particles, it is necessary to know not only the number density of each j-fold precursor, but also its time-age history. This makes the mathematical modeling much more complex and, for the time being, not amenable to practical solutions.

A further critical issue in any coagulative nucleation scheme is the specification of the $B_{i,j}$ rate coefficients according to the Fuchs formulation. To this end, the stability ratio $W_{i,j}$ is given as:

$$W_{i,j}=(\kappa r_{ij})^{-1}\exp(E_m/k_BT_e) \tag{53}$$

where E_m is the height of the potential barrier between two colliding particles, and κ is reciprocal of the thickness of the double layer. The total potential energy between unequal spherical particles is obtained from the Poisson-Boltzman (PB) equation with specifically imposed boundary conditions. Analytic solutions are available only with a number of approximations. For the case where particles have very different radii and very different surface potentials, all these approximations become inaccurate. Feeney et al. (1987a) obviated this limitation by introducing more precise solutions of the PB equation according to the Barouch-Matijevic (BM) (Barouch et al., 1985) theory. As a result, the coagulation between primary precursors and mature latex particles is much faster owing to an energy barrier lower than predicted by earlier approaches. The BM theory, however, is not universally accepted, and Overbeek (1988) has cast serious doubts on the validity of the solutions of the PB equation worked out by these authors.

While the overall potential energy between polymer particles certainly plays a key role in determining either the coagulation rate of primary particles or, as a result, the nucleation time, in our opinion, at this level of sophistication, much more attention should be drawn to the Hamaker constant that accounts for the van der Waals interactions in the attractive energy term. For polymer colloids this value can be obtained experimentally from the slope of the stability curve and the critical coagulation concentration (CCC) according to the Reerink-Overbeek (1954) equation. Tsaur and Fitch (1987) reviewed this methodology and found that for polystyrene latices the Hamaker "constant" increases regularly with increasing the surface charge density. This should not be surprising since the Reerink-Overbeek equation derived from approximate solutions for the PB equation. Accordingly, the Hamaker constant should be considered more likely as an adjustable parameter. It becomes then immaterial whether approximate or exact solutions of the PB equation are adopted for the evaluation of the height of the potential energy barrier E_m. Actually, the agreement between theory and experiment could always be found by slightly adjusting the Hamaker "constant." In this connection, for polystyrene latices the experimental values reported in the scientific literature span over more than one order of magnitude. According to the ECN scheme, this range of variation, while affecting only slightly the nucleation time T, has a profound effect on N_c.

The foregoing discussion strives to pinpoint how the simple extension of the behavior of model colloids according to the DLVO theory to very small, unstable latex particles typical of the nucleation stage, seems inadequate and open to a certain degree of arbitrariness.

Conclusions

A model that fully accounts for the time evolution of PSDs in the SE Interval I has been discussed, as well as the idea of extending to it the existing theories for the SE-Interval II. The approach is always based on a simple physical description of the underlying phenomena. The mathematical modeling follows then quite naturally this simple analysis. Two models taken into account are the well-known zero-one approach and the GF model. It has been shown that the zero-one model should be rejected for the PSD analysis, since it provides physically unreliable answers. This depends mainly on neglecting latex particles having more than one growing radical.

On the other hand, in the GF approach analytic solutions for the $\mathbf{n}_{\text{I}}(v,t)$ distribution are immediately available as time convolution integrals between the normalized formation rate of new latex particles and $\mathbf{n}_{\text{II}}(v,t)$. Owing to its mathematical formulation, the GF model provides analytic expressions also for the time evolution of the skewness of the PSD (as well as of any other cumulant). On this ground, it is possible to demonstrate that negatively skewed distributions are observed only with a monotonically decreasing nucleation rate. Simple algebraic relationships are derived for the skewness of the PSD at the end of the nucleation time T. This particular combination of moments depends on ρT only. However, for nucleation rates typical of micellar entry, negatively skewed PSDs are not possible from any practical standpoint.

This theoretical prediction is further confirmed when the experimental data from a presulfate-initiated styrene polymerization are interpreted on the grounds of the CN theory (Feeney et al., 1984): no agreement is found between theory and experiment. On the other hand, an acceptable fitting is obtained assuming a uniform decreasing formation rate of latex particles peculiar to micellar entry. Rather than suggesting evidences against a multistep nucleation scheme like CN, which *inter alia* is probably operative at surfactant concentrations below CMC, we strived to interpret the experimental data that combine, in an extended nucleation approach, the most relevant features of micellar, homogeneous and CN theories. The most interesting result is that the nucleation time T is much shorter than that predicted by previously reported models. As a result, most of the mechanistic information convoluted with the PSD is lost due to the stochastic broadening arising from particle growth processes.

Notation

a_s = area per molecule in Langmuir isotherm
A = $(k+sK)$, solubilized molecule into micelles
A_t = total polymer area
$B_{i,j}$ = Müller coagulation coefficient
b_s = Langmuir isotherm constant
c = pseudo-first order rate constant for mutual annihilation
$C_h(t)$ = homogeneous nucleation rate
C_i = concentration of solubilized ionic species
$\mathbf{c}(v, t)$ = source term vector (Eq. 1)
CMC = critical micellar concentration
C_{Mk} = monomer concentration in a k-fold precursor
d = intermediate variable, $(\rho+q)$
d_M = monomer density
d_p = polymer density
D_w = diffusivity of radicals in aqueous phase
E_m = height of the potential energy barrier
${}_1F_1(\ )$ = confluent hypergeometric function
$g(t)$ = normalized rate of formation of latex particles
G_k = formation rate of a k-fold precursor by monomer conversion
H = Hamaker constant
I = initiator, ionic strength
$\mathbf{I}_n(\ )$ = modified Bessel function of order n
j = inverse interparticle coefficient in the CN theory
j_{cr} = critical chain length
k = radical exit rate per particle
K = volumetric growth rate
$\mathbf{K}(v, t)$ = volume growth rate matrix (Eq. 1)
k_+ = polymer/surfactant adsorption rate constant
k_- = polymer/surfactant desorption rate constant
k^* = $(2\rho+k)$, K_{Surf}/ω
k_B = Boltzmann constant
k_d = initiator decomposition rate constant
k_e = rate constant for radical entry into particles
$k_e^{\max}$ = maximum entry rate constant (Eq. 34)
K_{eq} = micelles/aqueous phase equilibrium constant of A molecules
k_i = ith cumulant of the PSD
k_m = surface mass transfer coefficient
k_{me} = rate constant for micellar radical entry
k_p = propagation rate constant
K_{Surf} = k_+/k_-
k_{tw} = termination rate constant in aqueous phase
$\mathcal{L}$ = Laplace transform
M = critical degree of coagulation, monomer
M_o = monomer molecular weight
MC = surfactant micelle
$\bar{n}$ = average number of radicals per particle
N_A = Avogadro's number
$\bar{n}_{\text{Agg}}$ = micellar average aggregation number
N_c = number concentration of latex particles
n_i = number concentration of particles of size v and i radicals
N_i = number fraction of particles containing i radicals
N_s = particle surface sites occupied by a surfactant molecule
$\bar{n}_{ss}$ = average number of radicals per particle at stationary state
$\mathbf{n}(v, t)$ = normalized volume PSD
$\mathbf{n}^o(v)$ = normalized volume PSD of newly formed precursors
q = intermediate variable, $(\rho+k)$
r_i = radius of the ith precursor
R = reaction rate
r_{FH} = Flory-Huggins radius
r_m = micellar radius
s = Laplace variable
S = surfactant
S_p = surfactant adsorbed onto polymer particles
t = time
T = nucleation time
$[T^\bullet]$ = overall radical concentration
$T(\ )$ = top hat function
T_e = temperature of the emulsion
$U(\ )$ = unit step function
v, V = volume
V_A = hydrophobic volume of molecule A
V_p = volume of primary precursor
V_S = surfactant hydrophobic volume
$W_{i,j}$ = Fuchs stability ratio
x = dummy variable
X_A = average number of A molecules solubilized into micelles
Y_i = number concentration of i-fold precursors
z = t/T, ionic valence

Greek letters

α = average fraction of micellar ionization, movable point
α_{pw} = propagation probability in aqueous phase
β = k/K
β_e = coagulative entry switch
γ = activity coefficient
$\Gamma(\ )$ = gamma distribution function
δ = Stern layer thickness
$\delta(\ )$ = Dirac function
ϵ = error
ϵ_o = permittivity of the vacuum
ϵ_r = dielectric constant
η = water viscosity
Θ_s = fractional surface coverage by adsorbed surfactant
κ = inverse electric double-layer thickness
λ = intermediate variable
μ_i = ith moment of the PSD
ν = index
ρ = radical entry rate per particle
τ = intermediate time
τ_{Agg} = characteristic time of precursor coagulation
Ψ = generating function
ω = fraction of charged end groups on particle surface, molar water concentration
$\mathbf{\Omega}$ = kinetic coupling matrix (Eq. 1)

Subscripts

i, j, k = working indices
$1m$ = micellar primary precursor
w = aqueous phase

Literature Cited

Ahmed, S., M. S. El-Aasser, F. J. Micale, G. W. Poehlein, and J. W. Vanderhoff, "Rapid Measurement of Adsorption Isotherms of Emulsifiers on Latex Particles," *Polymer Colloids II*, R. M. Fitch, ed., Plenum, New York, 265 (1980).

Almgren, M., F. Grieser, and J. K. Thomas, "Dynamic and Static Aspects of Solubilization in Ionic Micellar Solution," *J. Amer. Chem. Soc.*, **101**, 279 (1979).

Almgren, M., and S. Swarup, "Size of Sodium Dodecyl Sulfate Micelles in the Presence of Additives: 2. Aromatic and Saturated Hydrocarbons," *J. Phys. Chem.*, **86**, 4212 (1982).

Almgren, M., "Kinetics of Excited State Processes in Micellar Media," *Kinetics and Catalysis in Microheterogeneous Systems*, M. Grätzel and K. Kalyanasundaram, eds., *Surfactant Science Ser.*, Vol. 38, M. Dekker, New York, 63 (1991).

Barouch, E., E. Matijevic, and T. H. Wright, "Double-layer Interactions of Unlike Spheres," *J. Chem. Soc., Faraday Trans.*, No. 1, **81**, 1819 (1985).

Behrman, E. J., and J. O. Edwards, "The Thermal Decomposition of Peroxodisulfate Ions," *Rev. Inorg. Chem.*, **2**, 179 (1980).

Blackely, D. C., "Theory of Kinetics of Compartmentalized Free-Radical Polymerization Reactions," *Emulsion Polymerization*, I. Piirma, ed., Academic Press, New York, 145 (1982).

Bucci, S., C. Fagotti, V. Degiorgio, and R. Piazza, "Small-Angle Neutron-Scattering Study of Ionic-Nonionic Mixed Micelles," *Langmuir*, **7**, 824 (1991).

Casey, B. S., I. A. Maxwell, B. R. Morrison, and R. G. Gilbert, "Establishing Mechanisms for Emulsion Polymerizations," *Makromol. Chem., Makromol. Symp.*, **31**, 1 (1990).

Coll, H., "Study of Ionic Surfactants by Membrane Osmometry," *J. Phys. Chem.*, **74**, 520 (1970).

Corrin, M. L., and W. D. Harkins, "The Effect of Salts on the Critical Concentration for the Formation of Micelles in Colloidal Electrolytes," *J. Amer. Chem. Soc.*, **69**, 683 (1947).

Corti, M., and V. Degiorgio, "Quasi-Elastic Light Scattering Study of Intermicellar Interactions in Aqueous Sodium Dodecyl Sulfate Solutions," *J. Phys. Chem.*, **85**, 711 (1981).

Dahanayake, M., A. W. Cohen, and M. J. Rosen, "Relationship of Structure to Properties of Surfactants: 13. Surface and Thermodynamic Properties of Some Oxyethylenated Sulfates and Sulfonates," *J. Phys. Chem.*, **90**, 2413 (1986).

Dunn, A. S., and L. C. H. Chong, "Application of the Theory of Colloid Stability to the Problem of Particle Formation in Aqueous Solutions of Vinyl Acetate," *Br. Polym. J.*, **2**, 49 (1970).

Emerson, M. F., and A. Holtzer, "On the Ionic Strength Dependence of Micelle Number," *J. Phys. Chem.*, **69**, 3718 (1965).

Emerson, M. F., and A. Holtzer, "On the Ionic Strength Dependence of Micelle Number: II," *J. Phys. Chem.*, **71**, 1898 (1967).

Feeney, P. J., D. H. Napper, and R. G. Gilbert, "Coagulative Nucleation and Particle Size Distributions in Emulsion Polymerization," *Macromolec.*, **17**, 2520 (1984).

Feeney, P. J., D. H. Napper, and R. G. Gilbert, "Periodic Nucleation Processes in Emulsion Polymerization Systems," *J. Colloid Interface Sci.*, **107**, 159 (1985).

Feeney, P. J., D. H. Napper, and R. G. Gilbert, "Surfactant-Free Emulsion Polymerizations: Predictions of the Coagulative Nucleation Theory," *Macromolec.*, **20**, 2922 (1987a).

Feeney, P. J., D. H. Napper, and R. G. Gilbert, "The Determinants of Latex Monodispersity in Emulsion Polymerizations," *J. Colloid Interf. Sci.*, **118**, 493 (1987b).

Feeney, P. J., E. Geissler, R. G. Gilbert, and D. H. Napper, "SANS Study of Particle Nucleation in Emulsion Polymerization," *J. Colloid Interf. Sci.*, **121**, 508 (1988).

Fitch, R. M., and C. H. Tsai, "Homogeneous Nucleation of Polymer Colloids. IV. Role of Soluble Oligomeric Radicals," *Polymer Colloids, Proc. Symp.*, R. M. Fitch, ed., Plenum Press, New York, 103 (1971).

Giannetti, E., "Comprehensive Theory of Particle Growth in the Smith-Ewart Interval II of Emulsion Polymerization Systems," *Macromolec.*, **23**, 4748 (1990).

Gilbert, R. G., and D. H. Napper, "The Direct Determination of Kinetic Parameters in Emulsion Polymerization Systems," *J. Macromol. Sci., Rev. Macromol. Chem. Phys.*, **C23**, 127 (1983).

Gilbert, R. G., B. R. Morrison, and D. H. Napper, "The Status of Nucleation Models in Emulsion Polymerization," *Polym. Mater. Sci. Eng.*, **64**, 308 (1991).

Goddard, E. D., and G. C. Benson, "Conductivity of Aqueous Solutions of Some Paraffin-Chain Salts," *Can. J. Chem.*, **35**, 986 (1957).

Hansen, F. K., and J. Ugelstad, "Particle Nucleation in Emulsion Polymerization. I. A Theory for Homogeneous Nucleation," *J. Polym. Sci., Polym. Chem. Ed.*, **16**, 1953 (1978).

Harkins, W. D., "A General Theory of the Mechanism of Emulsion Polymerization," *J. Amer. Chem. Soc.*, **69**, 1428 (1947)

Hiemenz, P. C., *Principles of Colloid and Surface Chemistry*, 2nd ed., M. Dekker, New York, (1986).

Krathovil, J., "Comments on Some Novel Approaches for the Determination of Micellar Aggregation Numbers," *J. Colloid. Interf. Sci.*, **75**, 271 (1980).

Lane, W. H., "Determination of the Solubility of Styrene in Water and of Water in Styrene," *Ind. Eng. Chem., Anal. Ed.*, **18**, 295 (1946).

Lang, J., and R. Zana, "Chemical Relaxation Methods," *Surfactant Solutions: New Methods of Investigations, Surfactant Science Ser.*, Vol. 22, R. Zana, ed., M. Dekker, New York, 405 (1987).

Lianos, P., and R. Zana, "Use of Pyrene Excimer Formation to Study the Effect of NaCl on the Structure of Sodium Dodecyl Sulfate Micelles," *J. Phys. Chem.*, **84**, 3339 (1980).

Lichti, G., B. H. Hawkett, R. G. Gilbert, D. H. Napper, and S. F. Sangster, "Styrene Emulsion Polymerization: Particle-Size Distributions," *J. Polym. Sci., Polym. Chem. Ed.*, **19**, 925 (1981).

Lichti, G., R. G. Gilbert, and D. H. Napper, "Theoretical Predictions of the Particle Size and Molecular Weight Distributions in Emulsion Polymerizations," *Emulsion Polymerization*, I. Piirma, ed., Academic Press, New York, 93 (1982).

Lichti, G., R. G. Gilbert, and D. H. Napper, "The Mechanisms of Latex Particle Formation and Growth in the Emulsion Polymerization of Styrene Using the Surfactant Sodium Dodecyl Sulfate," *J. Polym. Sci., Polym. Chem. Ed.*, **21**, 269 (1983).

Maxwell, I. A., B. R. Morrison, D. H. Napper, and R. G. Gilbert, "Entry of Free Radicals into Latex Particles in Emulsion Polymerization," *Macromolec.*, **24**, 1629 (1991).

Napper, D. H., and R. G. Gilbert, "Polymerization in Emulsion," *Comprehensive Polymer Science*, G. Allen, ed., Pergamon, Oxford, Vol. IV, 171 (1988).

Napper, D. H., and R. G. Gilbert, "Emulsion Polymerization: the Mechanisms of Latex Particle Formation and Growth," *Scientific Methods for the Study of Polymer Colloids and Their Applications*, F. Candau, R. H. Ottewill, eds., *NATO ASI Ser., Ser. C*, No. 303, Kluwer, 159 (1990).

Okubo, M., and T. Mori, "The Decomposition of Potassium Persulphate Used as Initiator in Emulsion Polymerization," *Makromol. Chem., Makromol. Symp.*, **31**, 143 (1990).

Okubo, M., M. Fujimura, and T. Mori, "The Acceleration of Decomposition of Potassium Persulfate in the Presence of Sodium Dodecyl Sulfate and Polymer Particles as a Model of Emulsion Polymerization System," *Colloid Polym. Sci.*, **269**, 121 (1991).

Ottewill, R. H., "The Stability and Instability of Polymer Latices," *Emulsion Polymerization*, I. Piirma, ed., Academic, New York, 1 (1982).

Overbeek, J. T. G., "Double-layer Interaction between Spheres with Unequal Surface Potentials," *J. Chem. Soc., Faraday Trans. 1*, **84**, 3079 (1988).

Patnode, W., and W. J. Scheiber, "The Density, Thermal Expansion, Vapor Pressure, and Refractive Index of Styrene, and the Density and Thermal Expansion of Polystyrene," *J. Amer. Chem. Soc.*, **65**, 3449 (1939).

Pearson, L. T., P. E. J. Louis, R. G. Gilbert, and D. H. Napper, "Studies of Particle Formation in Styrene Emulsion Polymerization Using 9-Vinyl Anthracene as a Probe Molecule," *J. Polym. Sci., Part A*, **29**, 515 (1991).

Perry, R. H., *Chemical Engineers' Handbook*, 6th ed., McGraw-Hill, New York (1984).

Priest, W. J., "Particle Growth in the Aqueous Polymerization of Vinyl Acetate," *J. Phys. Chem.*, **56**, 1077 (1952).

Ramkrishna, D., "The Status of Population Balances," *Rev. Chem. Eng.*, **3**, 49 (1985).

Reerink, H., and J. T. H. Overbeek, "The Rate of Coagulation as a Measure of the Stability of Silver Iodide Sols," *Discuss. Farad. Soc.*, **18**, 74 (1954).

Rhode, A., and E. Sackman, "Quasielastic Light-Scattering Studies of Micellar Sodium Dodecyl Sulfate Solutions at the Low Concentration Limit," *J. Colloid. Interface Sci.*, **70**, 494 (1979).

Richards, J. D., J. P. Congalidis, and R. G. Gilbert, "Mathematical Modeling of Emulsion Copolymerization Reactors," *J. Appl. Polym. Sci.*, **37**, 2727 (1989).

Schlueter, H., "Particle Formation and Catalyzed Agglomeration in Emulsion Polymerization," *Macromolec.*, **23**, 1618 (1990).

Smith, W. V., and R. H. Ewart, "Kinetics of Emulsion Polymerization," *J. Chem. Phys.*, **16**, 592 (1948).

Tsaur, S. L., and R. M. Fitch, "Preparation and Properties of Polystyrene Model Colloids," *J. Colloid Interf. Sci.*, **115**, 463 (1987).

Williams, R. J., J. N. Phillips, and K. J. Mysels, "The Critical Micelle Concentration of Sodium Lauryl Sulphate at 25°C," *Trans. Farad. Soc.*, **51**, 728 (1955).

Appendix A

By taking the Laplace transform with respect to time of Eqs. 2a and 2b we have:

$$s\mathcal{L}_o - G(v) = -\rho\mathcal{L}_o + q\mathcal{L}_1 \tag{1a}$$

$$s\mathcal{L}_1 - H(v) = \rho\mathcal{L}_o - q\mathcal{L}_1 - K(d\mathcal{L}_1/dt) \tag{1b}$$

where s is the Laplace variable conjugate to t, $\mathcal{L}_o$ and $\mathcal{L}_1$ are the Laplace transforms of $n_o(v,t)$ and $n_1(v,t)$, and $G(v)$, $H(v)$ are the PSDs at $t=0$ of particles having 0 and 1 radical, respectively. Summing up Eqs. 1a and 2a, it is possible to find a general expression for the Laplace transform of the $\mathbf{n}(v,t)$ distribution:

$$\mathcal{L}[\mathbf{n}(v,t)] = \frac{G(v)}{s+\rho} + \frac{1}{K}\frac{(s+d)}{(s+\rho)}H(v) + G(v)\frac{\rho}{(s+\rho)}\exp[-F(s)v] \tag{3a}$$

$$F(s) = \frac{1}{K}\left\{(s+q) - \frac{\rho q}{(s+\rho)}\right\} \tag{4a}$$

where $d=\rho+q$. The $G(v)$ and $H(v)$ distributions are not known unless in the very special case of $\mathbf{n}(v,0) = \delta(v)$. In this case, we have $G(v) = G\delta(v)$ and $H(v) = H\delta(v)$ where $G = q/(2\rho+k)$ and $H = \rho/(2\rho+k)$. Analytic expressions for $\mathbf{n}(v,t)$ are available through Laplace inversion of Eqs. 3a and 4a. For the simple case of a centered $\delta(v)$ Dirac function we obtain:

$$\begin{aligned}\mathbf{n}(v,t) = {} & G\exp(-\rho t)\delta(v) + \frac{1}{K}H\exp\left(\frac{-qv}{K}\right)\delta(t-v/K) \\ & + \frac{1}{K}\exp\left(\frac{-kv}{K}-\rho t\right)\left\{\left[H\left(\frac{\rho qv}{Kt-v}\right)^{0.5} + \rho qG\left(\frac{Kt-v}{\rho qv}\right)^{0.5}\right]\mathbf{I}_1\left[2\left(\frac{\rho qv}{K^2}\right)^{0.5}\cdot(Kt-v)^{0.5}\right]\right. \\ & \times U(t-v/K) + [qH+\rho G]\mathbf{I}_0\left[2\left(\frac{\rho qv}{K^2}\right)^{0.5} \left.\cdot(Kt-v)^{0.5}\right]U(t-v/K)\right\}\end{aligned} \tag{5a}$$

$U(x)$ represents the Heaviside unit step function. Equation 5a corrects a number of misprints which appeared in the original article by Lichti et al. (1981).

Appendix B

Under the assumptions of Eq. 6, in Interval I the ith SE Eq. 1 can be written as:

$$\begin{aligned}\frac{\partial n_i(v,t)}{\partial t} = {} & \rho[n_{i-1} - n_i] + k[(i+1)n_{i+1} - in_i] \\ & + c[(i+2)(i+1)n_{i+2} - i(i-1)n_i] \\ & - iK\frac{\partial n_i}{\partial v} + g(t)n_i^o(v)\end{aligned} \tag{1b}$$

Now, taking first the Laplace transform with respect to time t and introducing then the generating function for the $\mathcal{L}_i(s,t)$ transform of $n_i(v,t)$ (Giannetti, 1990), we have the following partial differential equation:

$$\frac{\partial\Psi}{\partial t} = \rho(x-1)\Psi + [k-Ax]\frac{\partial\Psi}{\partial x} + c(1-x^2)\frac{\partial^2\Psi}{\partial x^2} + g(t)\Psi^o \tag{2b}$$

where $\Psi(x,s,t) = \Sigma\mathcal{L}_i(s,t)x^i$

During SE Interval I we deal mostly with systems having a low number of radicals so that we can set $c=0$ replacing the exit rate constant by $(2\rho+k)$. Equation 2b reduces then to:

$$\frac{\partial\Psi}{\partial t} = \rho(x-1)\Psi + (k-Ax)\frac{\partial\Psi}{\partial x} + g(t)\Psi^o \tag{3b}$$

In Eq. 3b $\Psi^o(x,s)$ represents the generating function for the Laplace transforms of the PSDs of newly generated particles with i growing radicals. Since these particles are assumed at equilibrium with respect to their radical state occupancy, it follows that (Giannetti, 1990):

$$\Psi^o(x,s) = \mathcal{L}^o(s)\exp[\rho/A(x-1)] \tag{4b}$$

A general solution of Eq. 3b is Eq. 11, as can be easily proven by direct substitution, making then use of Leibnitz's rule of derivation under integration.

Manuscript received Aug. 27, 1992, and revision received Nov. 23, 1992.